Renewable and Sustainable Energy Reviews 25 (2013) 560–579

Contents lists available at SciVerse ScienceDirect

Renewable and Sustainable Energy Reviews

journal homepage: www.elsevier.com/locate/rser

Recycling of carbon dioxide to renewable fuels by photocatalysis: Prospects and challenges

Muhammad Tahir [1], NorAishah Saidina Amin *

Chemical Reaction Engineering Group (CREG)/Low Carbon Economy Group, Faculty of Chemical Engineering, Universiti Teknologi Malaysia, 81310 UTM, Skudai, Johor Bahru, Malaysia

ARTICLE INFO

Article history:
Received 20 July 2011
Received in revised form
31 March 2013
Accepted 12 May 2013
Available online 5 June 2013

Keywords:
CO_2 recycling
Photocatalysis
Hydrocarbon fuels
Sustainability

ABSTRACT

Energy crisis and threats of global warming has accelerated the thrust for new renewable energy resources. Recycling greenhouse gases seems eminently potential to produce sustainable fuels as well as to reduce carbon emission. Various possibilities for implementing low carbon economy drive by practicing phototechnology are reviewed in this paper. In particular, different challenges and applicable solutions for efficient and economical conversion of greenhouse gases to renewable fuels are discussed. The roles of key parameters such as types of reductant, reduction potential, pH of mixture, metal-loaded and supported catalyst on hydrocarbon yield and selectivity are also investigated. Various types of photoreactors and different challenges in the design are also elaborated. It was obvious that modification of semiconductor photocatalyst, optimum operating parameters and suitable photoreactor design are pertinent for efficient CO_2 reduction to sustainable hydrocarbon fuels. In view of the current scenario, there are ample opportunities for producing renewable fuels and establishing a sustainable carbon neutral cycle using phototechnology.

Contents

1. Introduction . . . 560
2. Prospects and developments in CO_2 recycling . . . 562
   2.1. Favorable recycling pathways . . . 562
   2.2. Fundamentals in photocatalysis . . . 563
   2.3. Progress towards sustainable hydrocarbon fuels . . . 566
3. Effects and roles of various factors in CO_2 recycling to hydrocarbons . . . 567
   3.1. Reduction potential . . . 567
   3.2. pH of mixture . . . 568
   3.3. Semiconductor conductance band . . . 569
   3.4. Metal modified catalysts . . . 569
   3.5. Catalyst type and support . . . 569
   3.6. Photoreactor design . . . 570
4. Advances in photoreactors for CO_2 recycling . . . 571
   4.1. UV light photocatalytic reactors . . . 571
   4.2. Solar photocatalytic reactors . . . 573
5. Recommendations . . . 576
6. Conclusions . . . 576
Acknowledgment . . . 576
References . . . 576

1. Introduction

Sustainable development depends directly on the availability of sufficient energy resources, consumption over restoration ratios and effects of energy on the environment. Consequently, rapid

* Corresponding author. Tel.: +60 7 553 5579; fax: +60 7 5588166.
E-mail addresses: bttahir@yahoo.com, mtahir@ciitlahore.edu.pk (M. Tahir), noraishah@cheme.utm.my, profnoraishah@yahoo.com (N.S. Amin).
[1] Permanent address: Department of Chemical Engineering, COMSATS Institute of Information Technology, Lahore, Pakistan.

1364-0321/$ - see front matter © 2013 Elsevier Ltd. All rights reserved.
http://dx.doi.org/10.1016/j.rser.2013.05.027

industrialization and modernization has amplified energy demands while fossil fuels have remained as the main source of energy, exacerbating critical social issues like security of energy supply and climate change [1,2].

Energy is essential for acquiring primary needs as well as for sustaining comfortable, modern life style. Energy needs are escalating due to better quality life, rapid industrialization and increase of populations [3–5]. Presently, world annual energy consumption is 13.95 terawatt (TW) which is expected to be higher than 50 TW at the end of this century. If such trends of energy consumption continue then all proven global oil reservoirs will be depleted within 42 years [6,7]. Therefore, an ever increasing world population hungry to consume more energy compared with limited non-renewable fossil fuels has created threats for course of collision [8]. Alternative renewable energy resources could provide sustainable energy necessary to sustain or improve the standards of living [9–11].

Nuclear technologies are considered attractive alternatives. However, the energy is unable to provide liquid fuels necessary for transportation and also to produce 10 TW per year, since it will consume all known uranium resources within 10 years [12]. In addition, this technology is unsafe, as demonstrated by the nuclear power plant disaster in Japan due to earthquake and tsunami in March, 2011. Utilization of biomass, however, offers ways for waste to wealth concept by converting forest, agriculture or municipal solid wastes to bioenergy or biofuels and can provide 7 to 10 TW of energy [13,14]. The wind can provide 2.1 TW while hydroelectric can provide an additional of 1.5 TW of energy. Cumulative energy from tides and oceans current would amount to less than 2 TW. The solar energy is considered freely available with average flux of 120,000 TW strikes on earth surface but it is diffuse and intermittent [15]. Therefore, in addition to these renewable energy technologies, other energy resources should be explored to provide sufficient energy for the 21st century and beyond.

Climate change is one of the primary concerns for humanity in the 21st century. The anthropogenic emissions of CO_2, mostly from combustion of fossil fuels, have widely been accepted as the main source of global warming. The concentration of CO_2 was increasing at a rate of ca. 1% per year but this increment per year has shifted to $>2\%$ over the last 25 years [16]. Many scientific studies reveal that CO_2 concentration has increased about 31% over the last 200 years. The global mean surface temperature has risen by 0.4–0.8 °C in the last century exceeding the base line of 14 °C [13,17]. If such trends persist, then the global temperature would be greater than 4.5 °C by the middle of this century. Given the growing demand for global energy with fossil fuels as the primary source, substantial reduction in CO_2 emissions is essential to stabilize its concentration. Moreover, for global temperature to stabilize the CO_2 global emission has to be reduced between 50 and 80% of the emission level reported in the year 2000 by 2050 [17,18].

Utilizing easily available and renewable carbon resource such as CO_2 for development of carbon based fuels is important for sustainability, since CO_2 is green and cheap, totally abundant, renewable feedstock and can mitigate global warming [19]. However, the biggest obstacle for establishing industrial processes based on CO_2 is its lower energy level. In other words, CO_2 is stable and higher energy is required to transform it into useful chemicals and/or fuels. During the last few years, various types of technologies have been under investigation for CO_2 reforming to carbon based chemicals and fuels namely, thermal reforming, plasma reforming and photoreduction [17].

In thermal reforming, CO_2 can be converted to synthesis gas (CO, H_2) through an endothermic process by supplying 247 KJ/mole of input energy at temperature range of 800–1000 °C and pressure of 8–10 bars over different types of catalysts [20–23]. The CO_2 reforming of CH_4 is explained by [24]

$$CH_4 + CO_2 \rightarrow 2CO + 2H_2 \quad \Delta H = +247\ \mathrm{KJ/mole} \tag{1}$$

In this reaction, the yield of syngas could increase with temperature; however, high temperature may affect catalyst stability. At higher temperature, more coke is produced which very likely is deposited over the catalyst surface causing catalyst deactivation and reactor clogging [24,25]. On the other hand, at the commercial level, fixed bed reactors are frequently employed for thermal reforming of CO_2–CH_4 to produce synthesis gas. The input energy required for endothermic reaction is supplied by natural gas combustion according [26]

$$CH_4 + 2O_2 \rightarrow CO_2 + 2H_2O \quad \Delta H = -800\ \mathrm{KJ/mole} \tag{2}$$

Eq. (2) reveals 1 mole of CH_4 releases 800 KJ of energy but only 70% of energy can be possibly utilized for efficient process. In this way, 0.44 mole of CH_4 will be necessary to reform 1 mole of CO_2 and 0.44 mole of CO_2 would be released to atmosphere. Therefore, to produce 2 mole of CO during CO_2 and CH_4 reforming, it would be necessary to utilize 1.44 mole of CH_4 with 0.44 mole of CO_2 emitted as greenhouse gas. Thus, a net 0.56 mole of CO_2 will be treated by consuming 1.44 mole of natural gas [27].

CO_2 reforming of CH_4 by plasma is considered a new technology that offers better alternatives compared to thermal catalytic processes. Contrary to catalytic reforming, plasma technology has advantages, since reaction takes place at lower temperature and pressure [28]. Nevertheless, higher input energy in terms of electrons and radicals production for reforming reactions is still a challenge. The reforming reactions through plasma are very complex. The simplified equations are given in [27]

$$CH_4 \xrightarrow{e^*\ or\ pyrolysis} C + 2H_2 \tag{3}$$

$$CO_2 \xrightarrow{e^*\ \mathrm{or\ pyrolysis}} CO + O \tag{4}$$

$$C + O \rightarrow CO \tag{5}$$

Eqs. (3) and (4) are highly endothermic reactions induced by thermochemical pyrolysis, while Eq. (5) is radical reaction. In plasma process, electrons, radicals and ions are produced by applying higher voltages using electricity, but on commercial scale this process is energized by combusting natural gas. As discussed in Eq. (2), during complete combustion of one mole of CH_4, about 800 KJ of heat energy is released. In efficient process, 42% of this energy can be converted to electricity and 67% of electricity is possible to be utilized in plasma reactions [27]. In this way, to get 2 mole of CO during CO_2 reforming, it would be necessary to burn 1.10 mole of CH_4 and 1.10 mole of CO_2 gas should be released to atmosphere. In addition, achieving higher efficiency inside a plasma reactor at the commercial level is quite challenging [29,30].

In recent innovations, the ubiquitous photocatalysis has gained increasing attention as it can operate at normal operating conditions. In photocatalytic CO_2 reduction to reusable hydrocarbon energy requirement for endothermic reaction could be provided through harnessing sunlight which is a green source of energy. In this technology, stability of catalyst and its performance is affirmed due to mild operating conditions. The photoreduction of CO_2 by using H_2O and/or CH_4 as reductant are stated in

$$CO_2 + H_2O \xrightarrow{hv,\ catalyst} CH_3OH + 3/2O_2 \tag{6}$$

$$CO_2 + 2H_2O \xrightarrow{hv,\ catalyst} CH_4 + 2O_2 \tag{7}$$

$$CO_2 + CH_4 \xrightarrow{hv,\ catalyst} CO + CH_3OH \tag{8}$$

Eqs. (6)–(8) revealed renewable fuels such as CO, CH_4 and CH_3OH can be produced in single step using solar energy. Hence, these

reactions affirmed phototechnology as the most attractive and a future hope for mitigation of greenhouse gas with production of green fuels for sustainable development [31]. However, there are certain challenges in practicing this technology as lower CO_2 conversion and selectivity have been reported [32,33]. To make CO_2 conversion approach economically practical and industrially scalable, research should focus on increasing the overall CO_2 photo-conversion efficiency and selectivity; thus ultimately efficient photocatalysts and reactors are needed. In this way, CO_2 recycling to renewable fuels using solar energy may imbues sustainable energy distribution in future without any net increase in greenhouse gas [34–36].

The objective of this paper is to review photocatalysis process for CO_2 recycling to hydrocarbon fuels. The main focus is to present the fundamentals in phototechnology, prospects in CO_2 recycling to hydrocarbon fuels and future challenges. The various factors that could affect CO_2 reduction process are critically discussed. The advances in photoreactors and recommendations to improve CO_2 reduction efficiency and selectivity are also deliberated.

2. Prospects and developments in CO_2 recycling

2.1. Favorable recycling pathways

Although phototechnology is most promising, there are certain fundamental pathways to obtain solar fuels as the final product. The necessary steps in CO_2 reduction to solar fuels include; (i) collection of solar energy, (ii) availability of feedstock (CO_2, H_2O), and (iii) photoreduction of feedstock to products. Solar energy is available in excess which can be captured and/or used as direct solar irradiations. However, for this purpose, efficient solar reactors are required. Besides this, UV light, energy from wind and other renewable energy resources could also be employed for photocatalysis.

Furthermore, CO_2 available in excess in atmosphere, could be captured and stored by employing efficient techniques [37]. For capturing CO_2, several possible ways including (a) chemical absorption, (b) physical absorption, (c) solid physical absorption, (d) cryogenic separation, (e) membrane separation, (f) and alkaline based salts are available Some novel ways of CO_2 capturing such as

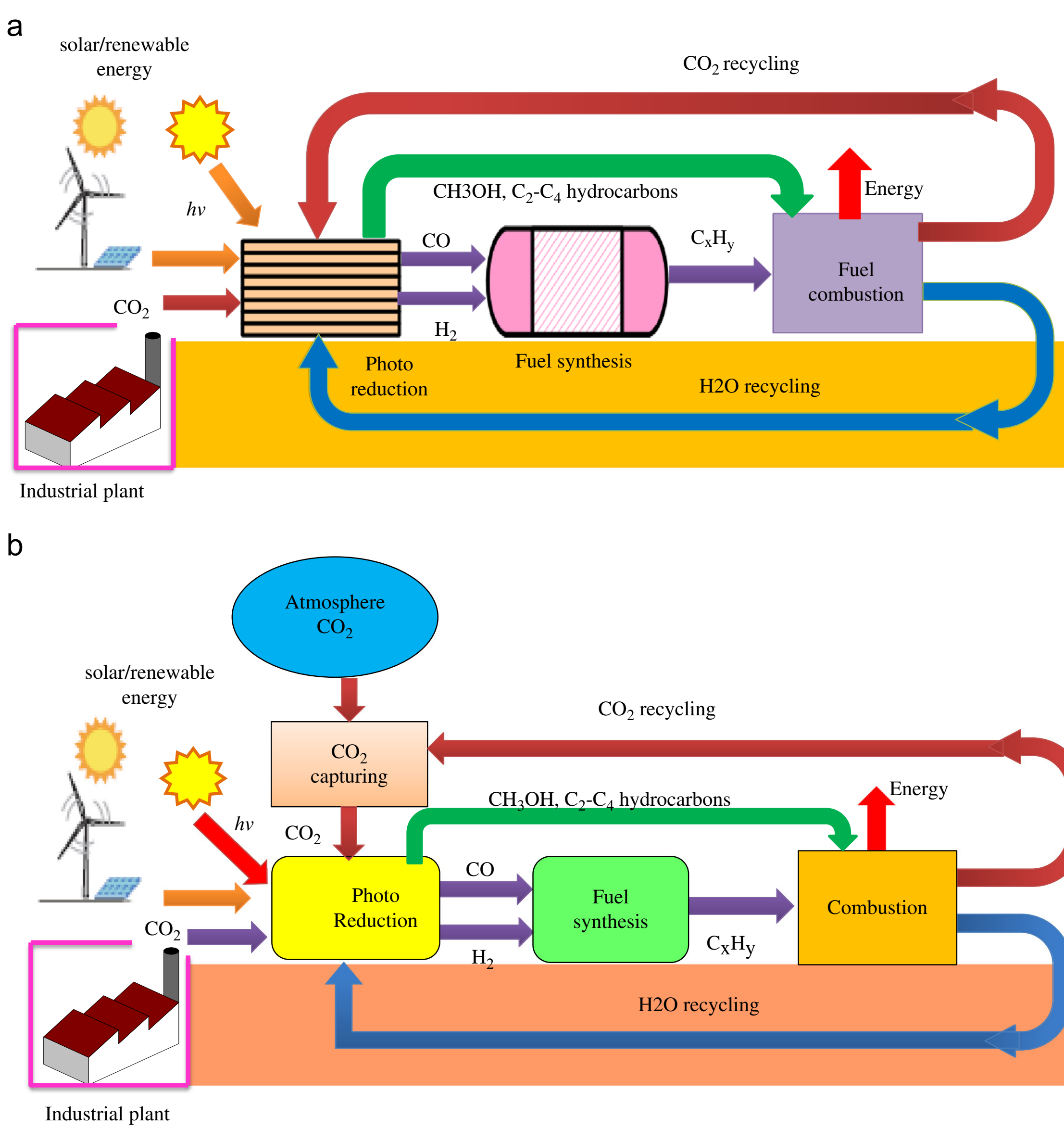


Fig. 1. Recycling of carbon dioxide to renewable fuels: (a) capturing and recycling of CO_2 from point source and recycling after combustion; (b) capturing and recycling CO_2 from point source and from atmosphere and recycling after combustion.

ammonia scrubbing, are being developed which would improve overall process efficiency [38]. However, efficient conversion of CO_2 feed stock to valuable chemicals under solar irradiations entirely depends on type of photocatalytic reactors. Therefore, highly scalable and novel reactors designs are critical for converting CO_2 to viable hydrocarbon fuels efficiently and economically.

The photocatalytic CO_2 reduction approaches helpful to produce hydrocarbon fuels are depicted in Fig. 1(a and b). CO_2 capturing from point source and photoreduction to hydrocarbon fuels is illustrated in Fig. 1(a). This approach will be useful mainly in power sector and industry as large scale point sources are available. The net carbon neutral cycle can be achieved by recycling CO_2 after hydrocarbon fuels combustion as well. On the other hand, input energy for CO_2 reduction could be employed using direct solar irradiations or using other renewable sources such as wind energy. This process can be tailored to generate CO. CO and H_2 can be combined to make synthesis gas used as feed stock for various processes including Fischer–Tropsch for liquid fuel synthesis. Further improvement in carbon neutral cycle could be possible by utilizing CO_2 from atmosphere in addition to recycling CO_2 from source, as illustrated in Fig. 1(b). Therefore, there are ample opportunities available to produce solar hydrocarbon fuels by recycling CO_2 but still efficient capturing and photoreduction technologies are critical.

Pertaining to sustainable development, complete CO_2 neutral cycle, indicating net zero carbon emission is depicted in Fig. 2 [39]. The artificial method of CO_2 recycling involve capturing CO_2 from the atmosphere or a point source and by subjecting to one or more chemical processes, it can be converted into value added products. These products could be used for energy production while completing the cycle obtained by capturing CO_2 released after combustion. However, external energy is required for CO_2 capturing and converting. Various physical methods will be employed for CO_2 capturing as discussed above. CO_2 conversion to CO or hydrocarbon fuels is much more energy intensive, hence solar or other renewable energy sources such as wind energy can be employed through photocatalysis or electro-catalysis. Hydrogenation of CO_2 over photocatalyst at normal temperature and pressure to make hydrocarbons such as CH_4, or oxygenated hydrocarbons like CH_3OH is also a viable approach. The hydrogen for this process can be derived from the sunlight driven water splitting process. The reversed water gas shift reaction will also be coupled with CO_2 reduction process through hydrogenation to form methanol and dimethyl ether. However, photoreduction of CO_2 through concentrated sunlight is one of the most promising approaches as it needed only CO_2 and water as the feed stocks if only hydrocarbons are to be produced. The synthesis gas produces during photocatalysis is used as feed stock for various processes including the Fischer–Tropsch for liquid fuel synthesis. These renewable fuels are compatible to replace petroleum based non-renewable fossil fuels and can either be supplied to industrial plants, transportation sector or to houses as source of energy. However, CO_2 photocatalysis to hydrocarbon fuels is still at its initial stages and significant developments are required to be scaled up commercially.

2.2. Fundamentals in photocatalysis

Photocatalysis is a process in which light radiations having energy equal to or greater than the band gap energy (E_{bg}) of a semiconductor strikes on its surface and generates electron (e^-)–hole (h^+) pairs. The photogenerated electrons and holes participate in various oxidation and reduction processes to produce final products. However, if the charges fail to find any trapped species on the surface or their energy band gap is too small, they recombine immediately releasing unproductive energy as heat [40]. In particular, the activity of heterogeneous photocatalysis depends on; (a) composition of reaction medium, (b) adsorption of reactants on semiconductor surface, (c) kind of

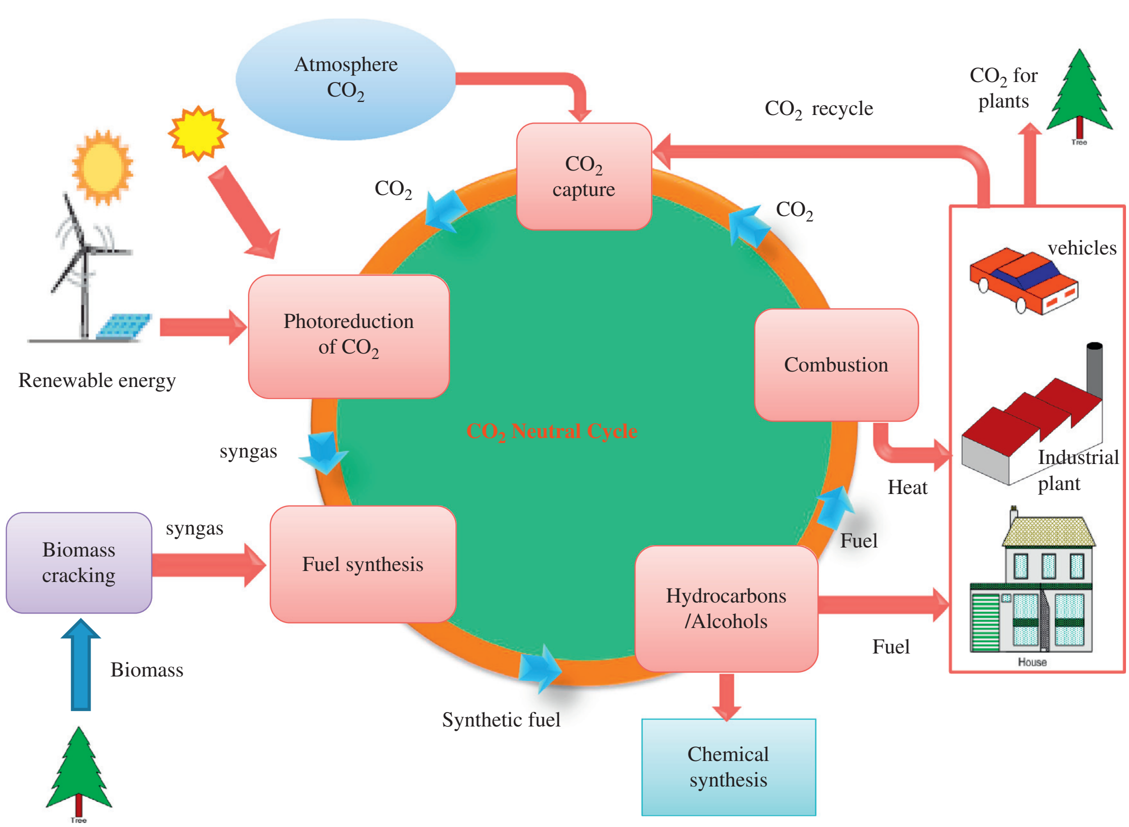


Fig. 2. Carbon dioxide neutral cycle with renewable methanol and liquid fuel production.

semiconductor and its crystallographic/morphological characteristics, and (d) ability of semiconductor to absorb UV or visible light [41,42].

During photoreduction process, several processes related to catalyst, interface, and donor–acceptor are involved as explained in Fig. 3. In catalyst related process, there is production of electrons and holes by absorbing photons. The lifetime of the charges is few nanoseconds only, therefore, several recombine immediately, and others participate in carrying various chemical reactions. Interface related process consists of transfer of electrons and adsorption on catalyst surface and mass transfer. In donor–acceptor related process, electrons and holes which escape from the excitation regions are trapped by adsorbed species, which become active and participate in various reduction and oxidation process.

Detailed explanation of photoreduction surface phenomenon for heterogeneous photocatalysis is presented in Fig. 4 [40,41]. The heterogeneous photocatalysis mechanism is very complex and many possibilities or reaction paths are possible. This depends on the life of charge particles i.e., if their energy band gap is lower

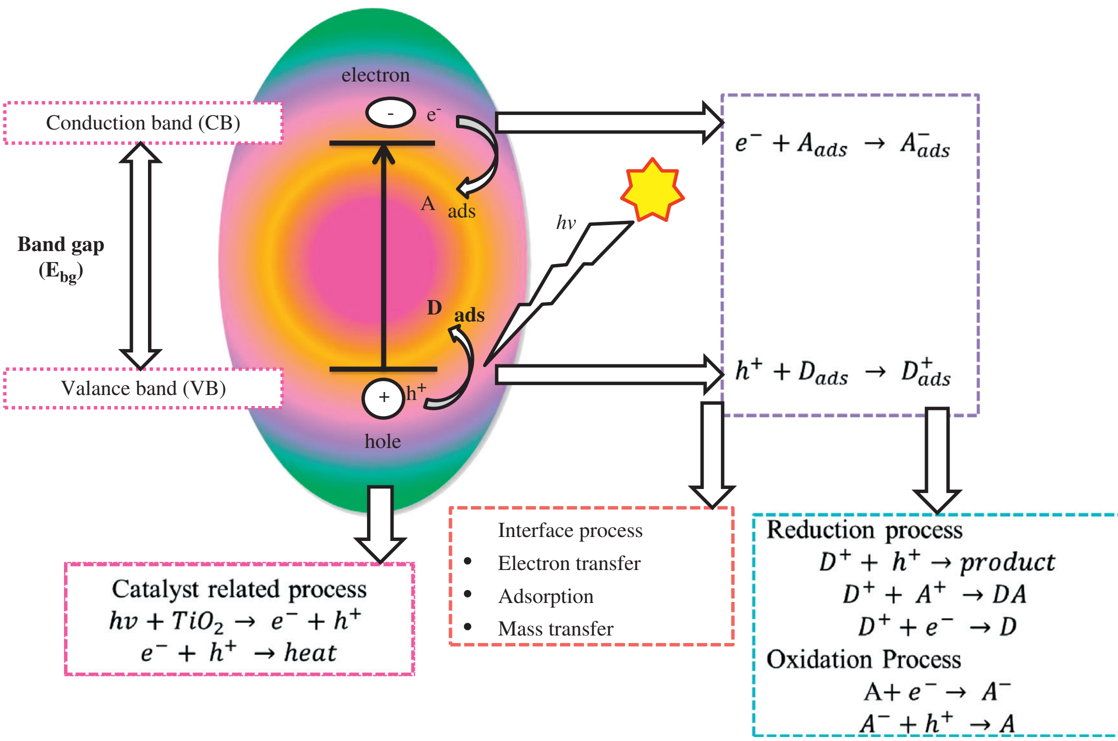


Fig. 3. Schematic representation of band gap formation and photocatalytic processes.

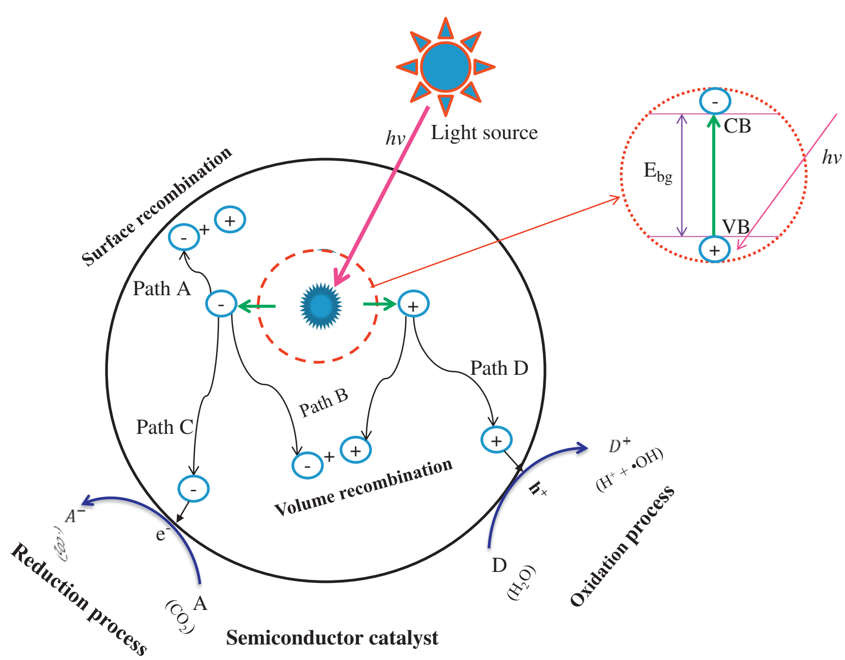


Fig. 4. Mechanism and pathways for photocatalytic oxidation and reduction processes on the surface of heterogeneous photocatalyst.

Table 1
Summary of photocatalytic CO_2 reduction literature over various types of photocatalysts.

Years	Reducant	Photocatalyst	Light source	*T*, *P*	product(s)	Reactor type	Comments	Ref.
1994	CO_2–H_2O	Cu–TiO_2	450 W-Xe-lamp	25 °C, 1 atm	Methane, ethylene	Stainless steel with quartz window	Trace amounts of methy alcohol, formaldehyde and CO were also produced.	[50]
1995	CO_2–H_2O	Cu/TiO_2	75-W, High pressure mercury lamp, $\lambda > 280$ nm	273–323 K, 1 atm	CH_4, CH_3OH, CO	Quartz cell	Addition of Cu promotes CH_3OH selectivity. TiO_2 (110) performs better than TiO (100)	[77]
1997	CO_2–H_2O	Pt/TiO_2-Y-zeolite	78-W, high pressure Hg lamp, $\lambda > 280$ nm	328 K, 1 atm	CH_3OH, CH_4	Quartz cell	Trace amounts of CO, C_2H_4, C_2H_6 and O_2 were also observed. The addition of Pt increases the selectivity of CH_4.	[51]
1997	CO_2–H_2O	TiO_2 powder	990 W Xe lamp,	*P*=6.5 MPa	HCOOH	High pressure stainless steel vessel	CO_2 was filled in high pressure tank and then irradiated for 30 h	[78]
1998	CO_2–H_2O	Cu, Ag, Au/p-Si	Tungston-Halogen lamp	25 °C, 1 atm	CO, H_2	H-shaped pyrex cell	Small amount of HCOOH was also produced.	[79]
1998	CO_2–H_2O	Ti-MCM-41 and Ti-MCM-48	High pressure mercury lamp, $\lambda > 280$ nm	328 K, 1 atm	CH_4, CH_3OH	Quartz cell connected with vaccum	TiO_2 played an important role for methanol selectivity.	[80]
1999	CO_2–H_2	Rh/TiO_2	500-W ultrahigh-pressure mercury lamp, λ=290–450	*T*=273 K, 1 atm	CO	Fixed bed quartz reactor	CH_4 was also produced and its selectivity increased by increasing Rh loading.	[81]
2002	CO_2–H_2O	TiO_2/SiO_2, Ti-MCM-41	100-W high-pressure Hg lamp	323 K, 1 atm	CH_4, CH_3OH	Quartz cell	Trace amounts of CO and O_2 were also produced. OH group played an important role in CH_3OH selectivity.	[82]
2003	CO_2–H_2O	Ti/Si-h-c (hexagonal and cubic)	100 W high pressure Hg lamp,	323 K	CH_3OH, CH_4	Quartz cell with flat bottom (88 cm^3)	The minor products like CO and O_2 were also observed. The yield increased linearly with time. The reaction was carried out in batch type mode.	[83]
2004	CO_2–H_2O	TiSBA-15	Mercury lamp	NA	CH_4, CH_3OH	NA	The absorption edges of TiO_2 shifted towards shorter wavelength. The yield of CH_4 was increased to 240 times and 4000 times for CH_3OH by using TiSBA-15 (2.4 M HCl) instead of TiO_2	[84]
2004	CO_2–CH_4	Cu/CdS –TiO_2/SiO_2	125-W, Ultrahigh pressure, Hg lamp	393 K, 1 atm	CH_3COCH_3 CH_3CH_3, CO	Quartz Fixed bed reactor	Conversion of methane 1.47% and CO_2 0.74% were achieved.	[85]
2004	CO_2–H_2O	TiO_2	λ=350 nm	NA	CH_4	Slurry reactor	CH_3OH and 2-roponal were also used as saturator.	[86]
2004	CO_2–CH_4	ZrO_2	500-W, Ultrahigh pressure, Hg lamp	293 K, 1 atm	CO, H_2,	Fixed bed, flat bottom reactor	The other products like HCHO and CH_3CHO were also observed.	[87]
2005	CO_2–H_2O	Cu/TiO_2	UV light	75 °C 1.05 to 1.4 bar	CH_3OH	Optical fiber photoreactor	CH_3OH yield increased with UV intensity and maximum achieved was 0.45 μmole g-catal.$^{-1}$ h^{-1} at pressure of 1.29 bars.	[88]
2005	CO_2–H_2O	CuO/TiO_2, 23 nm, 3% CuO, 45.8 m^2/g	UV lamp-10 W, 415–700 nm, 2.78 eV	NA	CH_3OH	Pyrex glass slurry reactor	Ethanol, propanol, acetone, and other hydrocarbons were also produced. CH_3OH yield increased up to 3% Cu loading.	[62]
2005	CO_2–H_2O	Ti-HMS	NA	328 K	CH_4, CH_3OH	Quartz cell	Ti with lower HMS content led to higher CH_3OH yield. Hydrophobical modification in Ti-HMS surface by fluorination led to higher selectivity of CH_3OH.	[89]
2006	CO_2–H_2O	TiO_2	UV lamp,	298 K	CH_4	Fixed bed quartz reactor	The yield of methane was 200 ppm. CO and H_2 were also found in the product in small amounts	[90]
2006	CO_2/CH_4, H_2	MgO	500-W, Ultrahigh pressure, Hg lamp	293 K, 1 atm	CO, H_2	Fixed bed flat bottom reactor	Formaldehyde and acetaldehyde were also used as reaction substrate. CO of 3.6 μmole was observed.	[91]
2007	CO_2–H_2O/H_2	TiO_2, ZrO_2	15-W, near-UV lamps, λ=365, 254 nm	43 °C, 1 atm	CH_4	Circulated reactor	Highest yield was obtained with H_2 and ZrO_2 catalyst. Traces of CO and C_2H_6 were also observed.	[92]
2007	CO_2–H_2O	NiO/$InTaO_4$	500 W halogen visible light, 2.6 eV, Wavelength= 465 nm	NA	CH_3OH	Pyrex reactor (slurry type)	CH_3OH yield increased with of NiO amount. Methanol yield obtained was 1.394 μmole g-catal.$^{-1}$ h^{-1} at 1% NiO loading.	[93]
2008	CO_2–CH_4	Ga_2O_3	300-W, Xe-lamp (220–300 nm)	473 K, 1 atm,	CO, H_2, C_2H_6	Quartz Fixed bed reactor	Other products such as C_2H_4, and C_3H_8 were also observed. Conversion is near 1.22%.	[94]
2008	CO_2–H_2O	Cu–Fe/TiO_2	150-W high pressure Hg lamp	25 °C, 1 atm	CH_4, C_2H_4	Catalyst coated optical fiber reactor	Presence of Fe co-doped on Cu enhanced C_2H_4 yield. Optical fiber reduction has higher yield than glass plate.	[95]
2008	CO_2–H_2O	TiO_2	200 W Hg/Xe-lamp	NA	H_2, CH_4	Slurry reactor	Initially, fast cumulative yield of CH_4 and after 4 h. there was no yield. Maximum yield was 21.5 μmole g-catal.$^{-1}$.	[96]
2008	CO_2–H_2O	Ag/TiO_2	8 W, Hg lamp 254 nm, 365 nm	NA	CH_4, CH_3OH	Batch stirred annular reactor	The yield of methanol was higher at 254 nm than 365. At 400 nm there was very low photocatalytic reduction of CO_2.	[97]
2009	CO_2–H_2O	CdS/TNT, Bi_2S_3/TNT	500 W Xe-lamp, 3.0 eV, 400–800 nm	298 K	CH_3OH	Continuous flow reactor	Modification of Titanium nanotubes (TNT) enhanced the yield of methanol. Higher yield (224.6 μmole g-catal.$^{-1}$ h^{-1}) was obtained by using Bi_2O_3, which was two times more than TNT.	[98]
2009	CO_2–H_2O	TiO_2	8-W, Hg lamp, $\lambda > 254$ nm	273 K, 110 KPa	CH_4, CH_3OH	Quartz tube reactor	Different particle sizes of TiO_2 were studied and found 14 nm as the optimum.	[99]
2010	CO_2–H_2O	NiO/InTaO4	100 W halogen lamp,	25 to 75 °C, 101 Kpa	CH_3OH	Pyrex glass optical fiber fixed bed reactor	With increase in temp, yield increased from 11.1 to 21 μmole g-catal.$^{-1}$ h^{-1}. With conc. Sunlight yield was only 11.30 μmole g-catal.$^{-1}$ h^{-1}.	[100]
2010	CO_2–H_2O	CdSe/Pt/TiO_2	300-W, Xe arc lamp, $\lambda > 420$ nm	25 °C, 1 atm	CH_4	Photocatalysis cell	CH_3OH, H_2, CO were also observed.	[34]

Table 1 (*continued*)

Years	Reducant	Photocatalyst	Light source	*T, P*	product(s)	Reactor type	Comments	Ref.
2010	CO_2–H_2O	SiO_2 supported Cu/TiO_2	Xe Lamp, 250 nm < λ < 400 nm	273 K, 1 atm	CO	Cylindrical continuous flow reactor built with stainless steel	Methanol, formaldehyde and formic acid were not measured. CH_4 appeared as a secondary product.	[101]
2010	CO_2–H_2O	Cu/TiO_2–SiO_2	Xe lamp	293 K, 1 atm	CO, CH_4	Fixed bed having catalyst on glass fiber	CO was primary product with TiO_2–SiO_2, but selectivity converted to CH_4 with Cu addition.	[101]
2010	CO_2–H_2O	Ag/TiO_2	8-W, Hg lamp, λ > 254 nm	273 K, 1 atm	CH_4, CH_3OH	Quartz tube reactor, slurry reactor	Yield of methane and methanol increased with Ag.	[102]
2011	CO_2–H_2O	ZnS-MMT	8-W, Hg lamp, λ > 254 nm	273 K, 1 atm	CH_3OH, CH_4, CO, H_2, O_2	Quartz tube reactor, slurry reactor	Highest yield was obtained when lamp was near the slurry surface.	[103]
2011	CO_2–H_2O	AgBr/TiO_2	150-W Xe lamp λ > 420 nm	7.5 MPa 5 h	CH_4, CO, CH_3OH, C_2H_5OH	Stainless steel slurry reactor	Methane (128.6 μmole g-catal.$^{-1}$) and ethanol (77.87 μmole g-catal.$^{-1}$) yields were highest. Ethanol (13 μmole g-catal.$^{-1}$) and CO (32 μmole g-catal.$^{-1}$) was also produced	[104]

and recombine immediately. However, if the charge particles have enough band gap energies to separate, then the following possibilities or paths are possible [37,42]:

a) The photoinduced charges move towards the surface of semiconductor, and transfer electrons or holes to adsorbed species. The electron transfer process is more effective if pre-adsorbed species already exist at the surface. At the surface, semiconductor can donate electron to reduce acceptors (path C), in turn a hole can transfer to the surface where an electron from donor species can combine with the surface hole, oxidizing donor species (Path D).
b) During charges transfer process, there is possibility of electron–hole recombination. Recombination of separated electron and holes can possible in the volume or at the surface of semiconductor with the release of unproductive heat.
c) Surface recombination (Path A) occurred when electrons and holes recombine on the semiconductor surface. On the other hand, if charges have the opportunity to recombine inside the semiconductor volume, then this process is called volume recombination (Path B).

2.3. Progress towards sustainable hydrocarbon fuels

Recycling CO_2 is a challenging task, since CO_2 is thermodynamically and kinetically stable that its reduction requires higher energy input. A lot of research has been conducted in CO_2 conversion to valuable chemicals [43–45] and fuels, while reaction involving only CO_2 and H_2O is more promising. Moreover, solar fuels drived during CO_2 reduction with H_2O can be used to develop CO_2 neutral cycle from the CO_2 balance point of view.

The earliest work on photo-electrochemical reduction of CO_2 to CH_3OH was reported by Halmann in 1978 [46] using electrochemical cell. Moving on, many researchers have investigated the use of different semiconductors to achieve visible light catalytic activities. Later in 1979, for the first time, photocatalytic reduction of CO_2 to various organic compounds namely CH_3OH, HCOOH, CH_4 and HCHO was studied by Inoue et al. [47] using both oxide and non-oxide photocatalysts such as TiO_2, WO_3, ZnO, GaP, CdS and SiC using H_2O as reducing agent illuminated by Hg and/or Xenon lamp.

Subsequently, many researchers have studied photocatalytic CO_2 reduction to fuels over various types of photocatalysts. Halmann et al. [48] reported the use of strontium titanate powder suspended in aqueous solution through which CO_2 was bubbled and illuminated by natural sunlight to produce HCHO, HCOOH and CH_3OH. Anpo et al. [49] reported the use of highly dispersed TiO_2 on glass for CO_2 reduction. Cu loaded TiO_2 powder was dispersed in CO_2 pressurized solution at ambient temperature by Adachi et al. [50]. The products found were CH_4 and C_2H_4 in Xe lamp illumination. In another report, photocatalytic reduction of CO_2 by H_2O vapor was studied using zeolite modified TiO_2 photocatalyst resulting in high gaseous CH_3OH selectivity [51]. Using Ti containing porous SiO_2 films, Ikeue et al. [52] reported the production of CH_4 and CH_3OH from CO_2 and H_2O mixture under Hg lamp irradiations. Another catalyst, Ru doped TiO_2/SiO_2 was used by Sasirekha et al. [53] for photocatalytic reduction of CO_2 to CH_3OH as well.

Recently, visible light photocatalysts have been under investigation for solar fuels production. The photocatalytic reduction of CO_2 to CH_3OH has been reported by Liou et al. [54], with production rate of 0.16 μmole g-catal.$^{-1}$ h^{-1} in which NiO doped $InTaO_4$ photocatalysts were illuminated under solar spectrum of wavelength 400 nm. Sato et al. [55] reported the p-type InP/Ru complex polymer hybrid photocatalyst for selective reduction of CO_2. The main product observed was HCOOH with trace amounts of H_2 and CO. In another study, Zhou et al. [56] reported ultra-thin and uniform Bi_2WO_6 square nanoplates for photocatalytic reduction of CO_2 and observed Bi_2WO_6 nanoplates were more efficient for reduction of CO_2 to CH_4 having yield rate of 1.1 μmole g-catal.$^{-1}$ h^{-1} with CH_3OH, O_2, H_2 and CO as secondary products. Efficient solar driven Ni and NiO modified N doped $InTaO_4$ photocatalyst was investigated by Tsai et al. [57] for efficient CO_2 reduction to CH_3OH. The maximum yield rate of CH_3OH reported was 162, 127.5 and 63.5 μmole g-catal.$^{-1}$ h^{-1} for Ni–NiO/$InTaO_4$–N, $InTaO_4$–N and $InTaO_4$ respectively.

Similarly, Li et al. [58] investigated the photocatalytic reduction of CO_2 to CH_4 using Pt loaded SiO_2− pillared HNb_3O_8 photocatalyst. The maximum yield of CH_4 was 3.75 μmole-g-catal.$^{-1}$ h^{-1} over 0.4 wt% Pt doped SiO_2−HNb_3O_8. A graphene photocatalyst-enzyme coupled photosynthesis system for production of HCOOH from CO_2 under solar energy was investigated by Yadav et al. [59]. The HCOOH production rate increased linearly under visible light irradiation. The maximum yield produced was 55.25 μmole h^{-1} by using CCGCMAQSP photocatalyst, while $W_2Fe_4Ta_2O_{17}$ gave a yield rate of 7.125 μmole h^{-1}. Visible light responsive plasmonic shaped Ag X: Ag (X 1/4 Cl, Br) nanoparticles were investigated by An et al. [60] for photocatalytic reduction of CO_2 to CH_3OH under visible light irradiation. Ag nanoparticles yield as much as 21 μmole g-catal.$^{-1}$ h^{-1} of CH_3OH was reported.

Among metals, copper (Cu) is the most studied metal. Cu doped TiO_2 is more efficient to convert CO_2 with H_2O to CH_3OH.

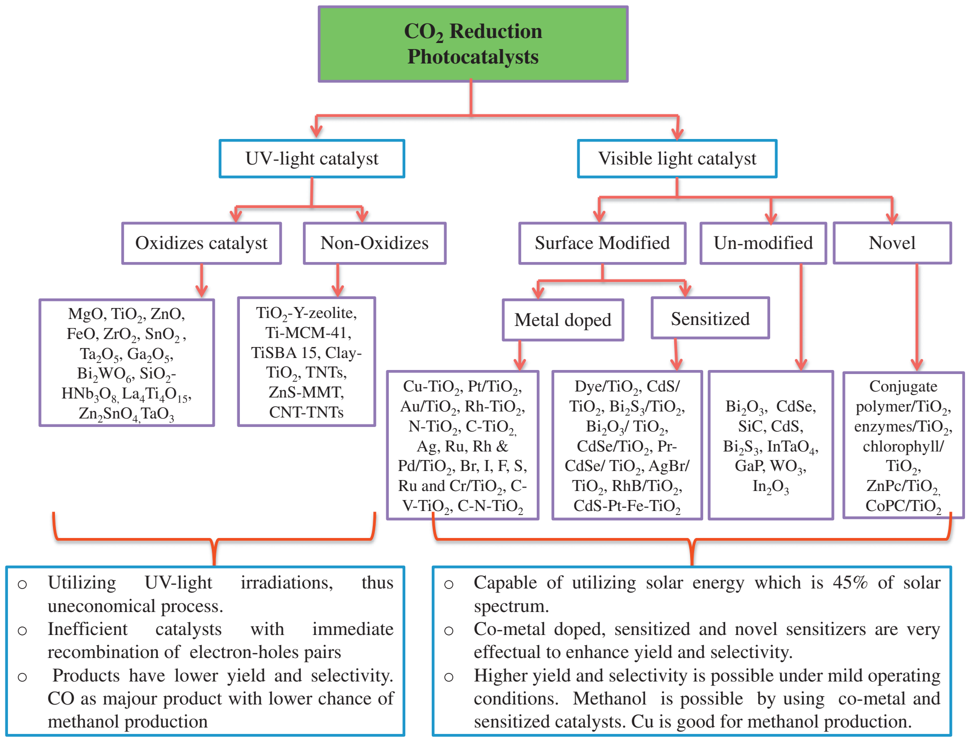


Fig. 5. Classification of UV and visible light CO_2 reduction photocatalysts.

Tseng et al. [61] used Cu–TiO_2 catalyst for CO_2 reduction to CH_3OH and found its efficiency two times higher than Cu–P25. Slamet et al. [62] synthesized Cu doped TiO_2 for photocatalytic reduction of CO_2 with H_2O and found CH_3OH as the main product. When 3% Cu was loaded and particle size of 23 nm employed, maximum CH_3OH yield obtained was 442.2 μmole g-catal.$^{-1}$ h^{-1} under visible light irradiations. Among transition metals, silver (Ag) is most widely used to get crystalline titania (Ag/TiO_2) for CO_2 reduction. Wu et al. [63] reported reduction of CO_2 to CH_3OH over Ag doped TiO_2 with yield rate was 4.12 μmole g-catal.$^{-1}$ h^{-1} over 1% Ag doped TiO_2. However, increasing Ag content increased CH_4 and CH_3OH yield rates up to the optimum loading. Au doped TiO_2 was investigated by Hou et al.[64] for photocatalytic CO_2 reduction with H_2O using green laser visible light at wavelength 532 nm. The yield of CH_4 achieved was 0.93 μmole m^{-2} using TiO_2 for 15 h which increased to 22.40 μmole m^{-2} with Au/TiO_2 used a 24 fold increment.

In non-metals, iodine (I) doped TiO_2 nanoparticles were synthesized by hydrothermal method and tested for photocatalytic CO_2 reduction to CO under visible light. The yield rate of CO increased at higher I content. 10 wt% of I in TiO_2 was found optimum for maximum CO production under solar irradiations. On the other hand, 5 wt% I–TiO_2 calcined at 375 °C showed lower activity than pure TiO_2 [65]. Similarly, Yui et al. [66] developed Pd doped TiO_2 by photochemical deposition method and tested for CO_2 reduction. The addition of 1 wt% Pd in TiO_2 resulted in product distribution from CO over TiO_2 to CH_4 over Pd–TiO_2 with smaller amount of CO and C_2H_6. The reuse of exhausted Pd–TiO_2 was found unfavorable to deliver the same.

Among dye sensitizers, photocatalytic reduction of CO_2 with H_2O into CH_4 was reported by Ozcan et al. [67] using dye sensitized TiO_2 and dye-Pt/TiO_2 photocatalysts under visible light irradiation. CH_4 yield increased with dye sensitizers Pt doped TiO_2 compared to Pt/TiO_2 and pure TiO_2 samples. Wang et al. [68] sensitized TiO_2 with ZnPc for photocatalytic CO_2 reduction with H_2O under visible light irradiations and observed CH_3OH as the main product. CH_3OH yield reached to 31 μmole g-catal.$^{-1}$ h^{-1} over 0.6 wt% ZnPc compared to bare TiO_2 having yield rate of 1.25 μmole g-catal.$^{-1}$ h^{-1}. With higher amount of ZnPc, the yield decreased gradually. Much larger enhancement factor i.e. 24.8 was achieved by using ZnPc as modifier.

Detailed literature survey about photoreduction of CO_2 using different semiconductors and reducing agents are explained in Table 1. It is obvious that CH_4, CH_3OH, and CO were the main products in majority of the work over different types of photocatalysts. The TiO_2 based photocatalysts were found more efficient than other types of photocatalysts and studied extensively. TiO_2 has lager band gap in the range of 3.0 eV to 3.2 eV and can absorb light with wavelength less than 380 nm. In response to shorter light absorption capacity, it can absorb only 3 to 4% of the total sun light that reaches the earth's surface [69,70]. The common strategies to enhance visible light response (VLR) and photoactivity of TiO_2 include: doping with metals and non-metals [71,72] and sensitization [67]. In addition, use of nanocarbons [73], graphene [74], enzymes [75] and novel sensitizer [76] have prevailed. The detailed literature on type of photocatalysts utilized for photocatalytic CO_2 reduction under UV and/or visible light irradiations with their characteristics are summarized in Fig. 5. It is obvious that a large variety of photocatalysts are tested for CO_2 reduction; among them surface modified and novel photocatalysts are of vital importance. Therefore, further work is needed to explore TiO_2 based photocatalysts due to numerous advantages such as low cost, excellent oxidizing power, abundantly available, corrosion resistance and stable. This could be the ultimate solution to develop sustainable phototechnology which could guarantee the production of economical solar hydrocarbon fuels.

3. Effects and roles of various factors in CO_2 recycling to hydrocarbons

3.1. Reduction potential

In photocatalytic CO_2 reduction, selection of reducing agent is vital, and reduction of species usually depend on their reduction

potentials. The reduction potential of H_2O to produce H_2 is considerably lower ($E^o_{red} = 0$ V) than the standard reduction potential of CO_2 to generate CO_2^- ($E^o_{red} = -1.9$ V) [105]. Therefore, during CO_2 reduction with H_2O, it would be more favorable to reduce H_2O instead of CO_2 because H_2O has lower reduction potential. Therefore, in photocatalytic CO_2 reduction with H_2O, in addition to other products H_2 should also be determined. If H_2 is not present in sufficient amount in the gaseous product mixture, then this would be good indication that H_2O is not competitng with CO_2 during the reduction process. However, if a large quantity of H_2 is generated, then it should be on the basis of thermodynamic consideration and photocatalytic activity should be re-evaluated under other operating conditions, preferably in the absence of liquid H_2O.

On the other hand, CO_2 reduction to CH_3OH, CH_4 and other hydrocarbons requires a reducing compound acting as hydrogen source. However, among different possibilities, the more challenging task is the use of H_2O as a reducing agent. The process of photocatalytic CO_2 reduction with H_2O is considerably more difficult than water splitting due to their redox potentials. To evaluate the possibilities of CO_2 reduction to CH_3OH or other hydrocarbon fuels, it is sensible to consider basic processes that could occur during CO_2 reduction with H_2O. The possible reactions in the reduction of CO_2 with H_2O in terms of thermodynamic reduction potentials versus normal hydrogen electrode (NHE) are explained by Eqs. are summarized in Table 2 [56,106–108].

Table 2
Summary of reduction potentials for half-cell reactions at pH 7 in aqueous solutions versus the normal hydrogen electrode.

Chemical equations		Thermodynamic potential, *V* vs NHE
$CO_2 + e^- \rightarrow CO_2^-$	(9)	−1.9
$2H^+ + 2e^- \rightarrow H_2$	(10)	−0.41
$CO_2 + 2H^+ + 2e^- \rightarrow HCOOH$	(11)	−0.61
$CO_2 + 4H^+ + 4e^- \rightarrow HCHO + H_2O$	(12)	−0.52
$CO_2 + 2H^+ + 2e^- \rightarrow CO + H_2O$	(13)	−0.48
$CO_2 + 6H^+ + 6e^- \rightarrow CH_3OH + H_2O$	(14)	−0.38
$CO_2 + 8H^+ + 8e^- \rightarrow CH_4 + H_2O$	(15)	−0.24
$H_2CO_3 + 2H^+ + 2e^- \rightarrow HCOOH + H_2O$	(16)	−0.166
$H_2CO_3 + 4H^+ + 4e^- \rightarrow HCHO + 2H_2O$	(17)	−0.050
$H_2CO_3 + 6H^+ + 6e^- \rightarrow CH_3OH + 2H_2O$	(18)	+0.044
$2CO_3^{2-} + 4H^+ + 2e^- \rightarrow C_2O_4^{2-} + 2H_2O$	(19)	+0.478
$2CO_3^{2-} + 3H^+ + 2e^- \rightarrow HCOO^- + 2H_2O$	(20)	+0.311
$2CO_3^{2-} + 8H^+ + 6e^- \rightarrow CH_3OH + 2H_2O$	(21)	+0.209
$2C_2O_4^{2-} + 2H^+ 2e^- \rightarrow 2HCOO^-$	(22)	+0.145
$HCOO^- + 5H^+ 4e^- \rightarrow CH_3OH + 2H_2O$	(23)	+0.157

It is obvious that multielectronic processes in Eqs. (10)–(15) are more favorable as they require less energy per electron transfer compared to monoelectron process (Eq. (9)). In Eqs. (10)–(15), each step requires a transfer of additional two electrons. Therefore, to study the feasibility of reaction occuring in photocatalytic process, the position of conduction and valance band edges are used as a simple tool to evaluate the possibility of potential reaction products. The photo-excited electrons can be utilized efficiently if the reduction potential of reaction is lower than the conductance band of semiconductor [109]. By comparing TiO_2 conductance band value (−0.50 eV) with that of thermodynamic potentials of reactions in Eqs. , it could be anticipated that the reactions in Eqs. are more favorable to produce CH_3OH and CH_4, since their reduction potentials are lower than the TiO_2 conductance band.

3.2. pH of mixture

Photocatalytic CO_2 reduction is more favorable under basic pH values and during its reduction, carbonates and bicarbonates may also be produced. However, carbonates and bicarbonates are good holes quenchers, are more stable compounds than CO_2 and it would be difficult to reduce them. In contrast, lower pH and higher proton concentrations lower the theoretical reduction potential of CO_2. However, higher proton concentration could enhance H_2 production by promoting H_2O splitting compared to CO_2 reduction. On the contrary, lower pH could shift the conduction band edge towards more positive and would be favorable to reduce CO_2

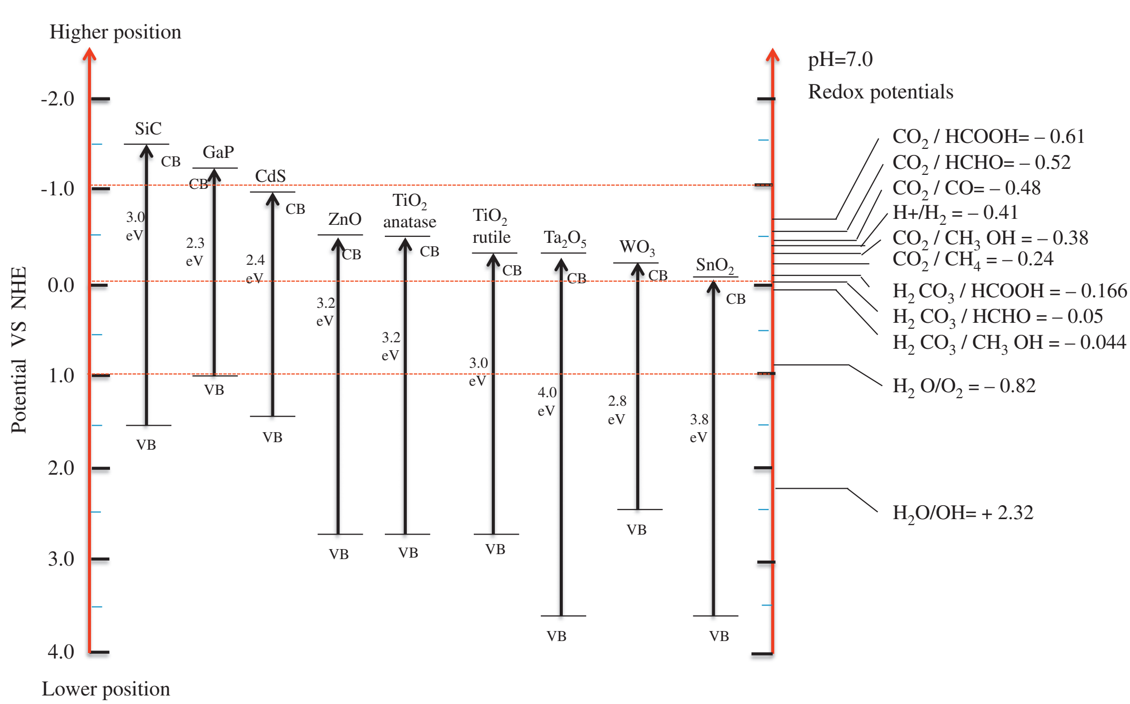


Fig. 6. Schematic representation of conductance band potentials of semiconductor and thermodynamic reduction potentials of various compounds measured at pH = 7 [47,56,106].

to CH_3OH through Eq. (14). Besides this, H_2CO_3 can be reduced to multiple products by Eqs. (16)–(18) and carbonate ions can also lead to different products by Eqs. (19)–(21). Molecular species and anions produced among various reactions could undergo different reactions Eqs. (22) and (23) for additional formation of CH_3OH.

3.3. Semiconductor conductance band

The effectiveness of semiconductors to transfer photo-induced electron toward adsorbed species depends on the semiconductor conductance band and redox potential of adsorbates. The band gap of semiconductor indicates its ability to absorb photons. Usually large band gap materials are most suitable for CO_2 reduction applications as they can provide enough redox potentials to execute chemical reaction. However, large band gaps require higher input energy [110]. The semiconductor band gaps in terms of their reduction potentials to reduce CO_2 with H_2O are depicted in Fig. 6 [47,106]. As a general role, the relative reduction potential of acceptor (adsorbed species) is thermodynamically required to be below (more positive) the conduction band of the semiconductor.

Aliwi et al. [111] utilized CdS for photocatalytic reduction of CO_2 at pH 6 and reported HCHO and HCOOH as the major products. The conductance band of CdS is about to −1.0 eV (E^o (red = −1.0 ev)) which is closer to values reported in Eqs. and more favorable for HCHO and HCOOH products. By using ZnS–CdS composites, HCOOH and CO were the main products due to their coductance band closer to Eqs. (14) and (15) [112]. Anpo et al. [113] tested various types of TiO_2 (anatase and rutile) photocatalysts and observed TiO_2 anatase was more favorable for CH_4 production while TiO_2 rutile exhibited higher efficiency for the formation of CH_4 and CH_3OH. Inoue et al. in 1979 reported reduction of CO_2 to CH_4, CH_3OH, HCHO and HCOOH by using TiO_2, WO_3, ZnS and CdS and suggested reduction of CO_2 to CH_4 is a multiple step reduction process.

3.4. Metal modified catalysts

Controlling recombination of photo-excited electron–hole pairs in semiconductor helps to maximize charge transferring toward adsorbed species. In different studies, several attempts are made to enhance charge separation process in order to improve CO_2 reduction efficiency [114]. One way to hinder charges recombination can be attempted through efficient monitoring of illumination. This could help to avoid excessive concentrations of electron (e^-) and holes (h^+) pairs, which ultimately will promote oxidation/reduction reactions [115]. On the other hand, recombination can be prevented by loading photocatalysts with metals and noble metals to function as charge-carrier traps. The defects and irregularities present on the surface and in bulk participate as charge carrier traps and suppress the recombination of electron and holes, as explained in Fig. 7(a and b) [110].

The addition of noble metals to semiconductor can change the photocatalytic properties due to change in semiconductor surface characteristics. The addition of metal to semiconductor increases the yield and selectivity of a particular product. The mechanism of metal surface modification and charge separation has been demonstrated in Fig. 8. Fig. 8(a) reveals that yield of CH_4 increased significantly with the addition of Au into TiO_2 structure. Fig. 8 (b) represents charge separation and interfacial redox reaction at Au nanoparticle modified TiO_2. Energy band alignment of anatase TiO_2, Au, and the relevant redox potentials of CO_2 and H_2O could efficiently produce HCHO, CH_3OH and CH_4 under visible illuminations.

Varghese et al. [21] reported CO_2 reduction to different hydrocarbon fuels using N and Cu co-metal doped TNTs under direct sunlight. The hydrocarbon production rate was 104 ppm cm^{-2} h^{-1} with Cu loaded N-TNTs (Fig. 8c). On the other hand higher production rates of H_2 and CO were observed by using Pt load N-TNTs with combined rate of 273 ppm cm^{-2} h^{-1} (Fig. 8d). Therefore, catalyst doping can enhance CO_2 reduction rate and product selectivity. Various types of dopants such as metals (Ag, Au, Rh, Pt, Cu, Ce, Pd, Sn and Ni), and non-metals (C, N, F, and S) could be employed to improve catalyst yield and selectivity. Recently, co-doped catalyst with both metal and non-metal ions exhibited remarkable potential as these catalysts are more effective to enhance photocatalytic activity compared to single or/non-metal doped photocatalysts [116,117].

3.5. Catalyst type and support

The limitation of photocatalytic activity for semiconductors can also be overcome by surface modification. Semiconductor surface modification has three advantages; (1) inhibiting recombination by increasing charge separation which ultimately increases efficiency, (2) enhancing wavelength response, and (3) increasing selectivity or yield of desired product. The design of molecular size catalysts within zeolite and other porous materials having micro pores is of special interest due to distinct physical and chemical properties [118]. Microstructured materials have many advantages including higher internal surface area, ion exchange capacities and porous structure allowing the molecules to diffuse into pores

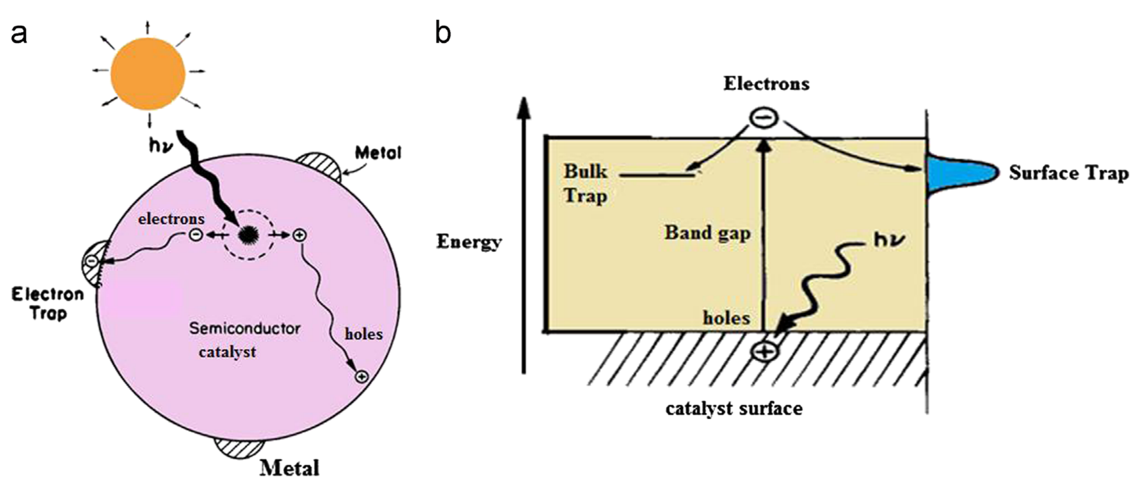


Fig. 7. (a) Metal modified semiconductor photocatalyst particles for electron trapping, (b) surface and bulk electron carrier trappings.

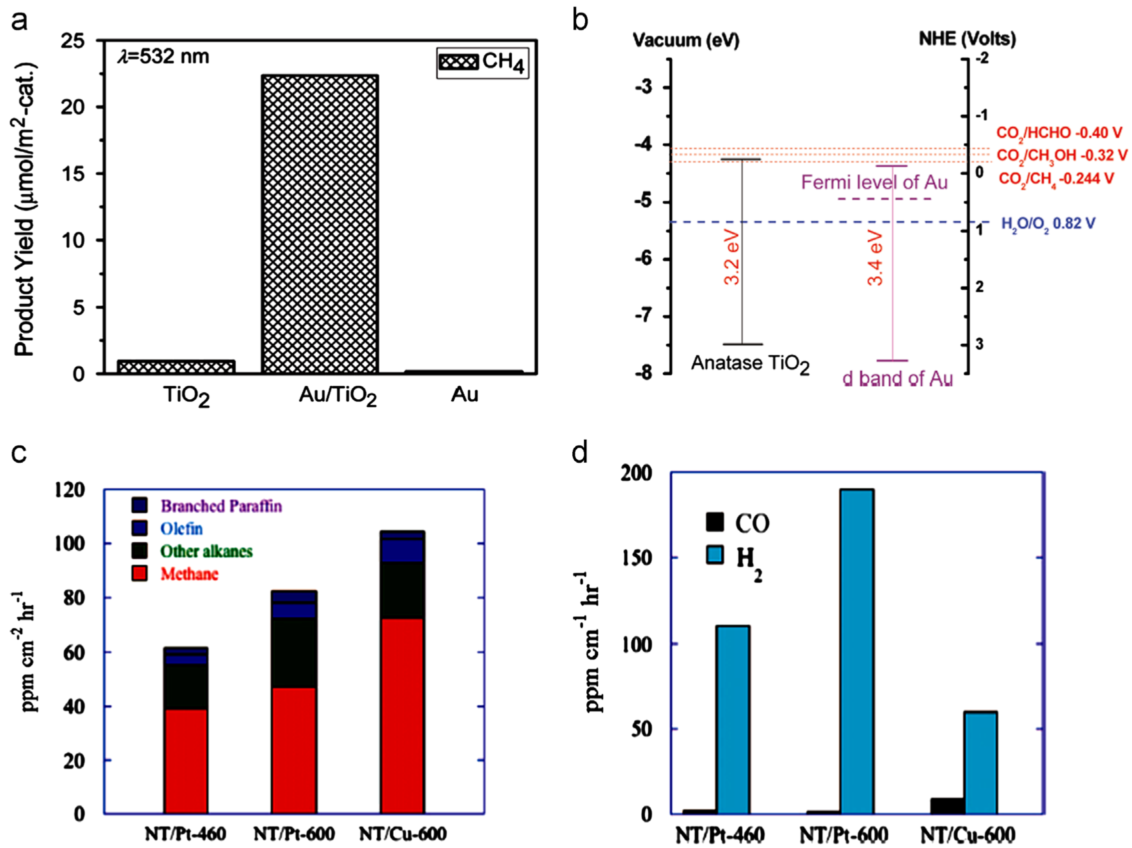


Fig. 8. Schematic illustrations of photocatalysts with their band gap potentials: (a) photocatalytic product yields (after 15 h of visible irradiation) on different catalytic surfaces, (b) energy band alignment of anatase TiO_2, Au, and the relevant redox potentials of CO_2 and H_2O under visible illumination; (c) nitrogen-doped titanium nanotube array films with Pt (TNT/Pt) and Cu (TNT/Pt) co-catalysts for hydrocarbon generation rate, (d) H_2 and CO generation rates [4]

cavities and remain intact during cluster growth [119]. Different types of sensitizers such as coupling semiconductors, carbon nanotubes, and some novel sensitizers could also be used to improve photocatalytic activity and selectivity under solar spectrum.

Zeolite materials have been tested in many studies due to their mesoporous structure. The photocatalytic CO_2 reduction with H_2O has been tested by many researchers using titanium oxide anchored within micropores of zeolites [51], Ti-MCM-41 and Ti-MCM-48 mesoporous zeolites [80] and Ti-beta zeolite [120]. Photocatalytic reduction of CO_2 with water was performed by using high surface area TiO_2 dispersed in porous silica coated as thin film and products such as CH_4, CH_3OH, CO and O_2 were detected [121]. Similarly CO_2 reduction with H_2O was conducted over highly dispersed TiO_2 and anchored TiO_2 [77,122].

In lower band gap semiconductor coupled with metals, Wang et al. [34] reported the photocatalytic reduction of CO_2 and H_2O using $CdSe/Pt/TiO_2$. It was observed that the hetero-structured materials are capable of sensitizing TiO_2 to shift its excitation band under visible light illumination at wavelength >420 nm. The maximum production yield rate was 48 and 3.3 ppm g-catal.$^{-1}$ h^{-1} for CH_4 and CH_3OH, respectively. Shi et al. [85] used coupled semiconductor Cu/CdS–TiO_2/SiO_2 for the photocatalytic reduction of CO_2 and CH_4 to oxygenated compound, and the maximum conversions of 1.47% and 0.74% for CH_4, and CO_2, respectively, with 92.3% selectivity of acetone were observed. Le et al. [123] modified the surface of sensitized TiO_2 with RhB and coated over Co/TiO_2 for photocatalytic reduction of CO_2 and H_2O. H_2 production rate of 98.9 μmole g-catal.$^{-1}$ h^{-1} was observed using RhB–Co/TiO_2 catalyst under the visible light irradiation. It was observed that H_2 production rate has increased to six times using RhB–Co/TiO_2 than Co/TiO_2.

The analysis and comparisons of different types of surface modified photocatalysts to reduce CO_2 into hydrocarbon fuels is demonstrated in Fig. 9. It is obvious from Fig. 9(a) [124] that TiO_2 can be used efficiently as visible light responsive (VLR) photocatalyst to develop solar hydrocarbon fuels based technology by modifying its surface with dopants and/or with sensitizers. It could be seen that TNTs surface modified with sensitizers like Bi_2S_3 has a higher yield than TNT but lower than Bi_2S_3. The overall concept of this progressively enhanced yield is linked with efficient production and utilization of electron and hole pairs. On the other hand, higher production rate of hydrocarbon fuels like CH_3OH was observed by using metals doped sensitizer/ TiO_2 composites. By investigating the overall trend in CO_2 reduction to solar hydrocarbon fuels, an obvious increment trend in yield of CH_3OH could be seen. The yield rate was in the order of dopant-sensitized TiO_2 > co-doped TiO_2 > metal modified TiO_2 as depicted in Fig. 9(b).

3.6. Photoreactor design

The photoreactor differs from traditional chemical reactors. The physical geometry of photoreactor is significantly important to insure photons are collected effectively. The photoreactor operational parameters like temperature and pressure have less importance compared with effective absorption of photon on catalyst surface. The renewable technology and mitigation of CO_2 by photocatalysis has led interest in this technology, but this field is

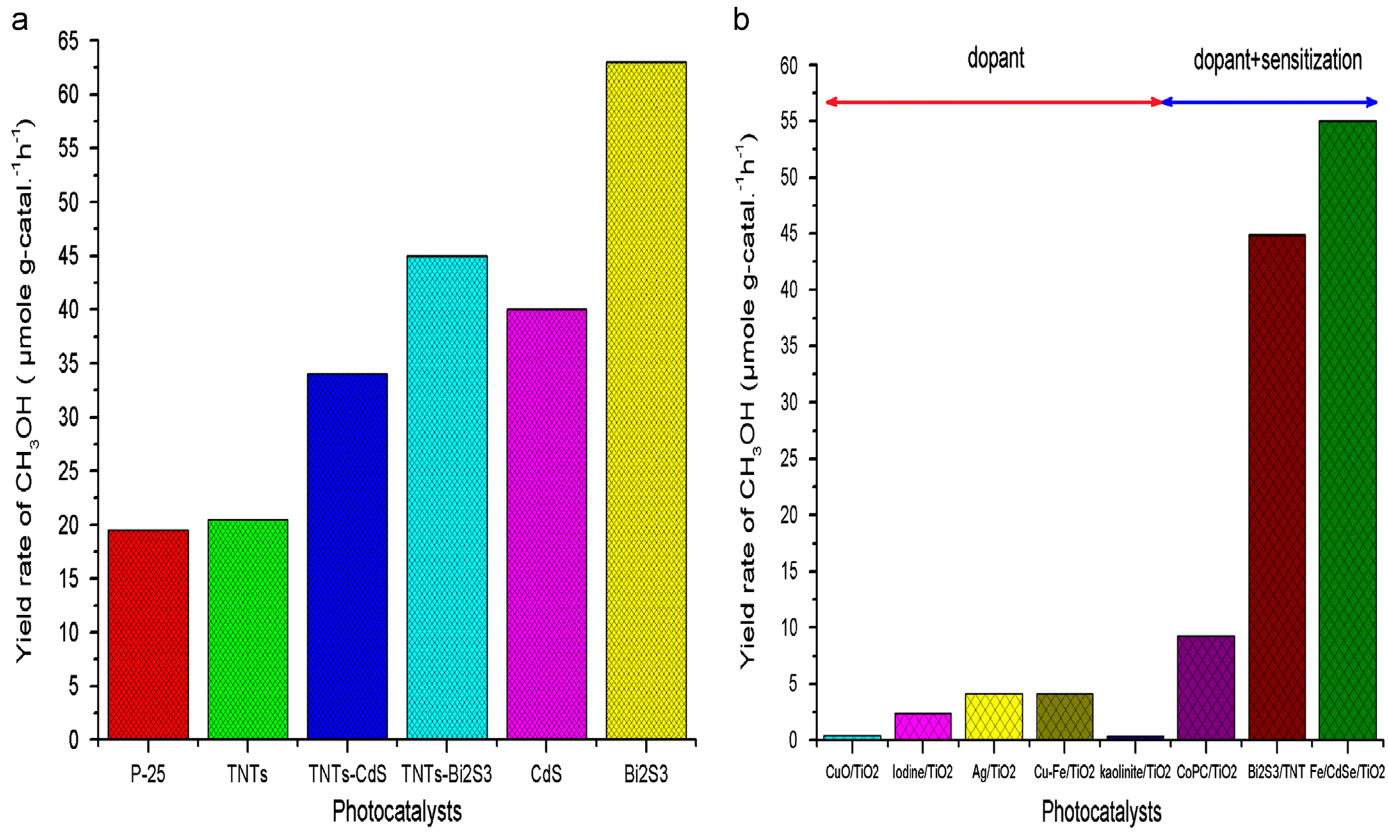


Fig. 9. (a) Comparison of average production rate of CH_3OH from CO_2 reduction using different type of TiO_2 based photocatalysts, (b) performance of different types of TiO_2 photocatalysts surface modified with dopants and/or sensitizers for photocatalytic reduction of CO_2 and H_2O.

relatively new and photoreactor design has not been standardized yet and various designs have been considered [125].

For industrial applications, several design parameters like photoreactor geometry, efficient photocatalyst for absorbing of light radiation, efficient utilization of radiant energy, transmissions of radiant energy on catalyst surface, longer life time of electron and holes and efficient interaction between reactants are necessary to be optimized. The successful design of photoreactor must have ability for increasing the number of photon absorbed per unit area per unit volume as well as efficient utilization of electrons and holes for improved photocatalytic activity [41].

4. Advances in photoreactors for CO_2 recycling

In photocatalysis applications, CO_2 conversion and yield rates could only be enhanced if equal importance is given to both catalysts and reactors. Several parameters are important in photoreactor design but not included in conventional chemical reactors including selection of radiant source, source efficiency, spectral distribution, shape and dimensions as well as design of irradiant devices including mirrors, reflectors, windows and their construction materials, shape and cleaning procedure.

In addition to reactor design strategies and efficient catalyst, there are a number of operating variables that affects the rate and extent of chemical reaction transformation including semiconductor concentration, reactive surface area, and particle aggregative size, concentration of electron donors and acceptors and incident light intensity. However, photoreduction of CO_2 can be practiced by using both solar and ultraviolent radiations in various types of reactors [41]. The general classification of UV and solar reactors under consideration has been depicted in Fig. 10.

4.1. *UV light photocatalytic reactors*

Various types of UV light photocatalytic reactors have been practiced in the last decades for photocatalytic CO_2 reduction. The two phase system can be gas–solid or liquid–solid and are operated in either fluidized bed or fixed bed mode. Three phase systems are the combination of gas, liquid and solid and are operated in different flow patterns. The most common types operated under three phases systems are trickled bed, bubble flow fixed bed, high velocity flow and continuous stirrer tank reactors.

The most common types of reactors under investigations for CO_2 reduction are slurry reactors, fixed bed reactors and annular/bubble flow reactors. Slurry type reactors have been practiced since the last three decades using photocatalytic oxidation process. Various studies have been conducted in laboratory scale by dispersion of catalyst in aqueous phase (slurry). For the first time in 1979, Inoue et al. [47] worked on photocatalytic reduction of CO_2 to different products by using slurry reactor in which catalysts were suspended in water. During the period of 1980 to 2000, slurry type reactors were under consideration for reduction of CO_2 using UV or visible light irradiation [48,126,127]. Such types of reactor design faces various problems such as presence of fine solid phase catalyst which led to fouling of radiation source, less active surface contact area, and additional cost during the separation of fine catalyst particles.

During the last 10 years, there is gradual development in design of photocatalytic reactors for reduction of CO_2 under UV/Visible light irradiation. However, the most widely used reactors are fixed bed, surface coated annular type, and optical fibers. In fixed-bed reactor, the catalyst is coated or anchored on the reactor wall for efficient absorption of light radiation. In such reactors, fluid flow regime approaches to plug flow tends to achieve higher

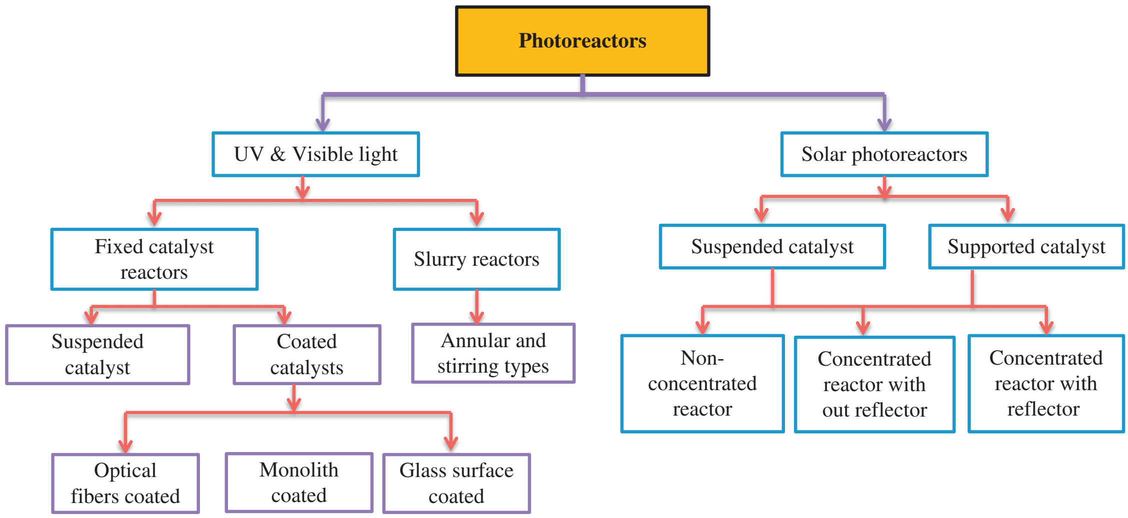


Fig. 10. Classification of UV and solar photocatalytic reactors.

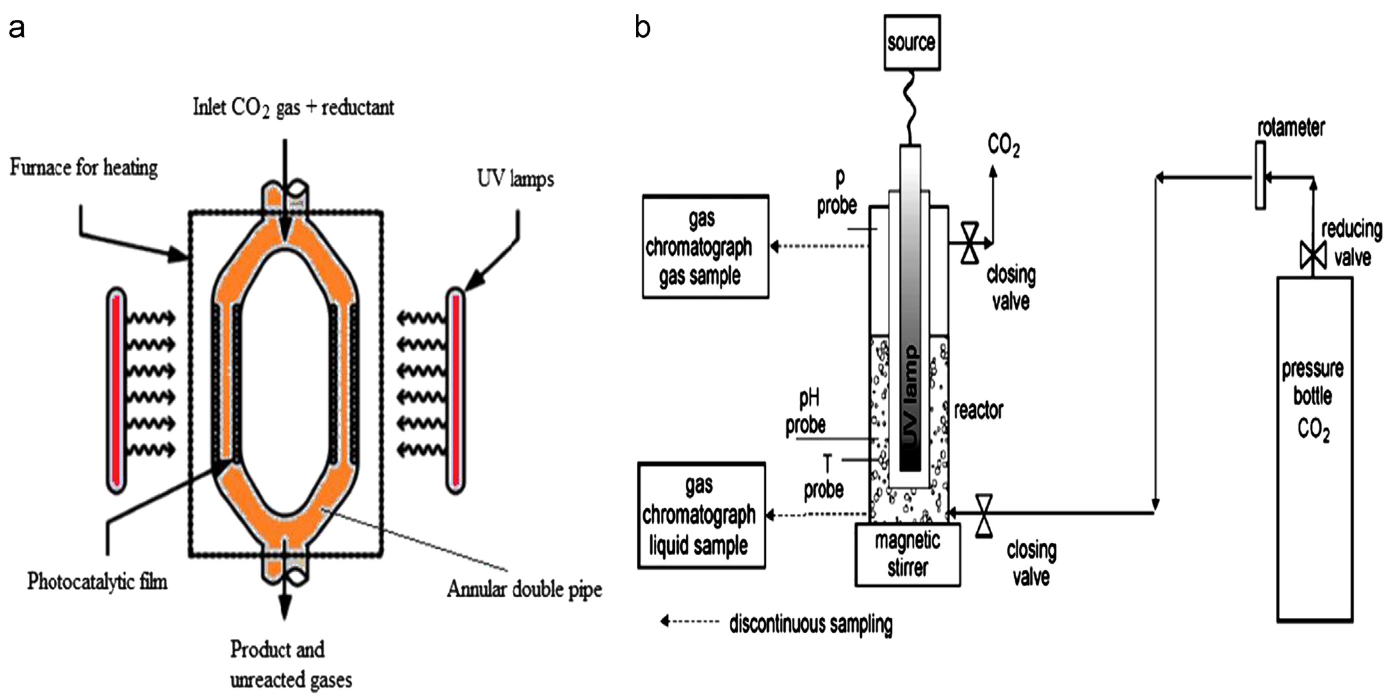


Fig. 11. (a) Outlines of gas flow and light reflection in optical fibers, (b) images of photoreactor with optical fibers.

conversion per unit mass of catalyst. The advantages of fixed-bed reactors are the low pressure drop which enables such system to be operated under reduced cost and also catalyst stability. Such types of reactors still provide lower contact exposure to light area for maximum conversion and yield rates.

The annular type reactors usually have two concentric cylinders in which catalysts are coated, packed or suspended. The source of light for photocatalytic reaction can be located at the center or around the reactor. In general, the cross section of the reactor tube is small to accommodate higher gas velocity for ensuring products desorbed on the surface are removed effectively. Multitubes reactor consists of cylindrical vessel with hollow glass tubes externally coated with photocatalysts. Such reactor configurations are similar to shell and tube type heat exchangers [128–131]. The source of light for photocatalytic reaction can be located around the reactor or at the center. Fig. 11(a) illustrates the source of light around the reactor tubes while the heating source could also be used to maintain temperature. The schematic batch stirred annular reactor is shown in Fig. 11(b) in which CO_2 was continuously bubbled through water while illuminated separately by using lamp in the inner cylinder.

In 2005 Jeffrey et al. [88], for the first time used the optical fiber photoreactor for reduction of CO_2 and H_2O. The schematic representation of optical fiber photocatalytic reactor is depicted in Fig. 12. Although optical fibers can deliver light efficiently and uniformly, yet they have various disadvantages. Among them are lower adhesion strength, relatively low surface area and only 20–30% of the reactor volume is available for photocatalysis [54,132].

Recent advancement in phototechnology showed monolith reactors have various advantages compared to commercial reactors. Utilization of monolith having microchannels with higher light interaction surface area can increase the conversion and yield rates. In 2011, Liou et al. [54] for the first time used monolith photoreactor for photocatalytic reduction of CO_2 with H_2O

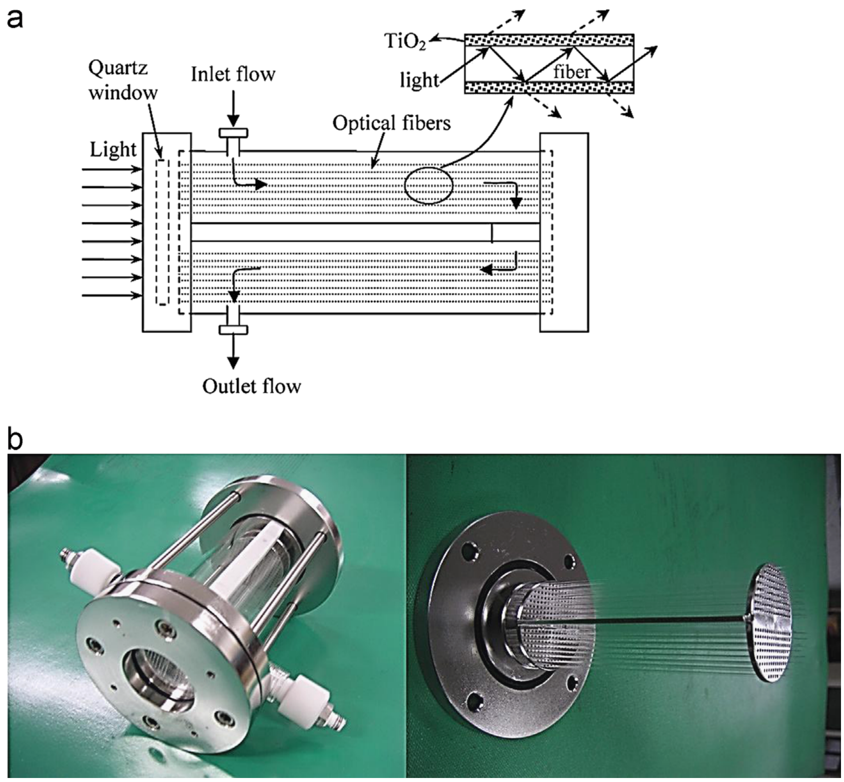


Fig. 12. (a) Schematic representation of annular reactor with the lamp outside the shell, (b) schematic of batch annular stirred reactor for CO_2 reduction [103].

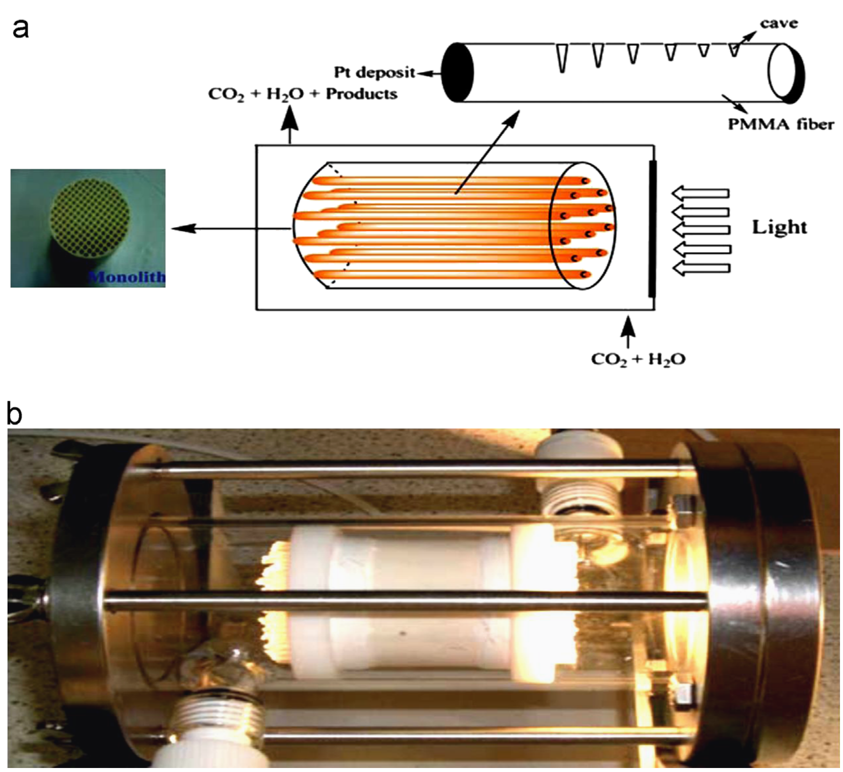


Fig. 13. (a) Schematics of monolith reactor and illumination fibers, (b) internally illuminated monolith photoreactor for CO_2 reduction with H_2O.

to CH_3OH. The schematic of monolith photoreactor is shown in Fig. 13. The illumination inside the reactor was promoted by inserting optical fibers inside the monolith channels. The catalyst was coated inside the channel by dip-coating. Comparisons of different types of UV and/or visible light photocatalytic reactors with their limitations are summarized in Table 3.

4.2. Solar photocatalytic reactors

The use of artificial UV light ultimately increases total annual operating cost of photocatalytic process. This drawback prompts the idea to harness solar radiation for industrial applications. From the strength of solar flux that reaches the earth's surface,

Table 3
A summary of different types of UV photocatalytic reactors and their limitations.

Category	Type	Characteristics	Limitations
Three phase	Slurry reactors	• They are the combination of gas–liquid–solid phases. • They can be operated in different flow patterns. • Experiments are conducted by dispersion of catalyst in aqueous phase (slurry). • They can be operated in fixed bed mode or continuous flow patterns.	• Separation of catalyst from mixture is quite difficult. • The presence of fine solid in slurry leads to scale up and fouling of light source. • Have less active contact surface for photocatalysis. • Additional cost during separation of fine particles. • Reduction of CO_2 with lower conversion and yield rates of desired products. • Additional cost in case of continuous stirring of slurry.
	Fluidized reactors	• Catalyst and reactants are in fluidized form. • Vigorous agitation of solid by passing fluid resulting in efficient heat and mass transfer rates within the bed. • High photocatalytic activity.	• Erosion by abrasion of particles and attrition of the catalyst. • Separation of catalyst from mixture is quite difficult. • Operational cost of catalyst separation. • Fluidized approach decreases the economical validity of the system.
Two phase	Fixed bed reactors	• They have gas-catalyst or liquid-catalyst phases. • Operated in either fixed bed or fluidized bed mode. • Catalyst is usually suspended on the reactor bottom. • High conversion per unit mass of catalyst. • Catalyst in powder or pellets could be used.	• Lower exposure of catalyst to light irradiations. • Lower quantum yield and mass transfer on the catalyst surface. • Lower conversion and yield rates. • Usually studied in batch mode due to lower conversion of CO_2. • In continuous flow system yield rates of products will be difficult to measure.
	Bubble flow fixed bed reactors	• Consists of bed of catalyst and coaxial lamps radiation source. • Random packing with relatively small particles. • Packing is particularly quartz glass coated with thin layer of photocatalyst. • Reductant flow through gravity and separated at bottom. • CO_2 is flowed upward in opposite direction. • High mass transfer rate and catalytic activity.	• Lower interaction surface area between catalyst and light irradiations. • Higher pressure drops and erosions of catalyst. • Lower conversion and yield rates. • Difficult to control operating conditions. • Maintaining reaction temperature is difficult. • Only suitable at normal operating temperature and pressure.
	Annular reactors	• Usually have two concentric cylinders coated or packed with semiconductor catalyst. • Source of light can be located at center or around the reactor. • In tubes, higher gas velocity for ensuring products desorbed from the surface are removed effectively.	• In fixed bed tubes, possibilities of uneven or partial light distribution. • Lower surface area for catalytic reactions. • In fixed bed tubes, high pressure drop. • Lower conversion, and yield rates.
	Optical fiber photoreactors	• Catalyst is arranged with certain structure or arrangements. • Higher interaction between irradiations and catalyst surface. • Efficient light distribution throughout the reactor. • Higher conversion and yield rates. • Lower operational costs. • Lower pressure drop and more stability of catalyst.	• Lower adhesion strength of catalyst. • Relatively low surface area for chemical reactions. • Only 20–30% of reactor volume is available for photocatalysis. • Uniform coating of fibers is very complex and special methods are demanded.
	Monolith photoreactors	• Efficient distribution of light over the catalyst surface. • Higher volume to surface area ratios • Fluid flow regime tends to plug flow and low pressure drop. • High loading and stability of catalyst. • Most suitable for gas–solid systems which particularly have higher feed rates. • Higher conversion and selectivity.	• Only reflector type light source can be used. • Coating of catalyst inside channel demands specific methods like dip coating. • Lower catalyst adhesion on walls and could be eroded under high flow rates.

approximately 10% can be utilized effectively for photocatalytic applications. Efficient utilization and solar spectrum harvesting have important considerations in solar energy applications. There are several articles about the design of solar photocatalytic reactors for wastewater treatments and these reactors can be applied for photoreduction of CO_2 with certain modifications. The basic difference in design of wastewater and CO_2 treatment system is that wastewater reactor are designed for organic and biological destruction in aqueous solution while for CO_2 system, CO_2 is dissolved in water or other solvents before destruction for useful products.

Solar reactors have two basic types: suspended and supported photocatalyst under concentrated and non-concentrated sunlight reactors which have further classification as listed in Table 4. In concentrating reactor, solar light is concentrated and gathered in a photocatalytic reactor with the help of reflecting surface. Non concentrating reactors consume more sunlight because they capture diffuse UV light as well as direct solar radiations. In addition, non-concentrated systems can function as solar collectors as well as photocatalytic reactors [91,125].

The parabolic trough reactor is concentrating type units consist of tubular reactor section and parabolic reflecting section.

Table 4
Reactor classifications for solar photocatalytic reactions.

Category	Suspended photocatalyst	Supported catalyst
Concentrating reactors	• Parabolic trough reactor • Falling film reactor	Parabolic trough reactor
Non concentrating reactor without reflectors	• Solar pond • Tubular reactors • Inflatable tube reactor • Pressurized tube reactor • Flat plat reactor • Trickle down flat plat reactor • Double skin sheet reactor • Falling film reactor	• Flat plate reactor • Trickle down flat plate reactor • Thin film fixed bed reactor
Non concentrating reactor with reflectors	Compound parabolic collecting reactor	• Tubular reactor • Fiber optic cable reactor

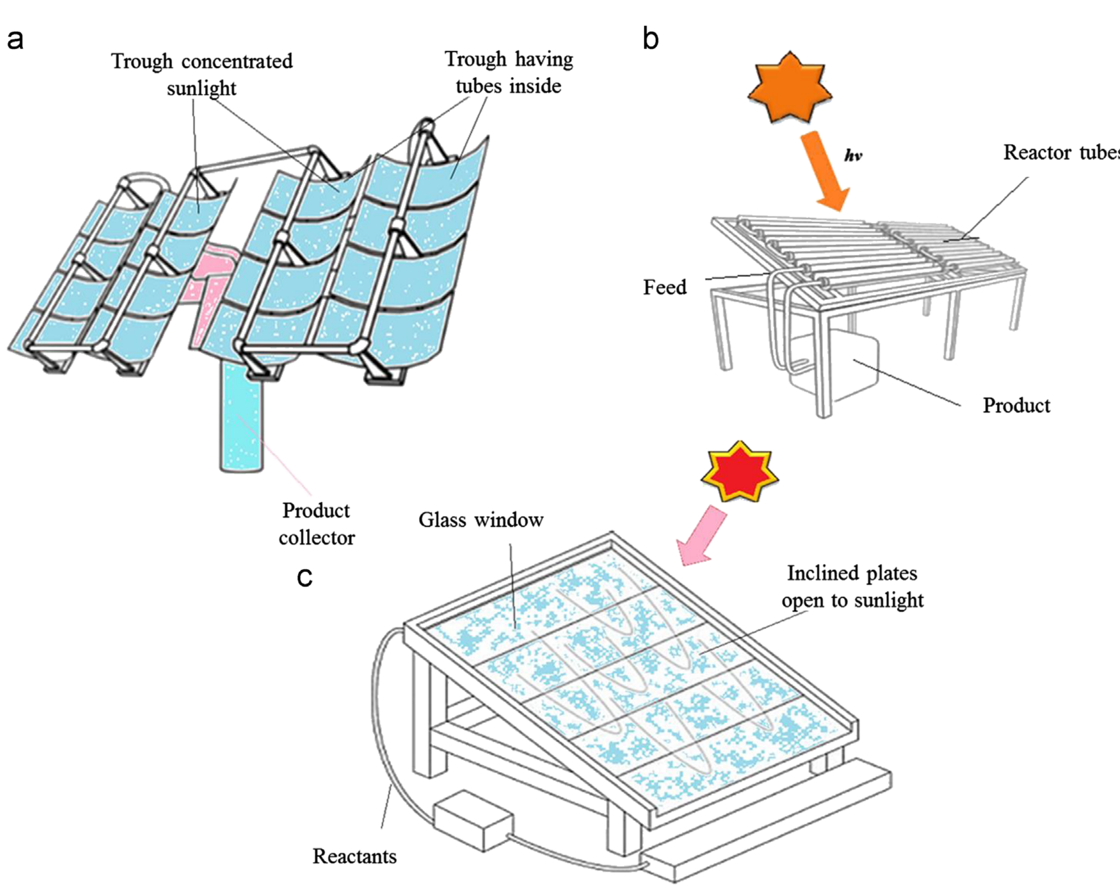


Fig. 14. (a) Parabolic trough type solar photocatalytic reactor [133]; (b) compound trough type solar photocatalytic reactor; (c) inclined plate reflector solar photocatalytic reactor [125].

Such types of reactors are designed by using long tube, reflective, parabolic surface for concentrating solar radiation on a transparent tube place along the parabolic focal line and trough in which the reactant fluid flow [133]. The configuration of parabolic trough type reactor is shown in Fig. 14(a). In such type of reactors, the catalyst is either suspended as fine particle in reactant fluid or supported on reactor tubes. In parabolic trough reactors, surface area of absorber tube is substantially lower than reflecting surface, which helps to concentrate photons and light intensity on photocatalyst. On other side, compound parabolic rectors are more efficient than trough type and their configuration is shown in Fig. 14(b). The greater advantages of compound parabolic trough are that reactor geometry allows the indirect light to be reflected on absorbed tube surface [125].

The design of concentrating parabolic and non-concentrating compound parabolic reactors is taken from commercial solar thermal reactors, but they do not represent a potential design. The photocatalytic systems depends on operational parameters that differs from solar thermal processes like mass transfer between photocatalyst and reactant fluid, ensuring efficient illuminations of photocatalyst and being able to handle catalyst effectively. The most suitable reactor which fulfills all these requirements is inclined plate reactor, as shown in Fig. 14(c). The basic design consists of flat, inclined surface upon which reactant

fluid flows as thin film. The photocatalyst is supported on the surface of inclined plates, provide larger illuminated surface area and could efficiently harvest higher solar energy. This design is simple, efficient, uses low cost material and can be practiced for diverse applications [134,135].

5. Recommendations

It is obvious recycling of CO_2 by utilizing solar energy could be fruitful to produce economical and sustainable hydrocarbon. However, improving the lower yields during CO_2 reduction is a challenging task ahead. The selection of efficient photocatalysts and appropriate design of photocatalysts are some of the observed limitations that needed focus. The operating parameters could also be optimized to maximize conversion and yield rates. Therefore, applying basic engineering and scientific approaches should achieve the goal to recycle CO_2 to sustainable fuels and overcome the constraints.

In order to develop efficient CO_2 reduction phototechnology, equal importance should be given to basic pillars of photocatalysis i.e. photoreactor and catalyst. The design of photocatalytic reactor is efficient only if there is a good interaction between four phases (liquid, gas, solid and light) for gas–liquid systems and three phases (gas, solid and light) for gaseous systems. The distribution of catalyst and light inside photocatalytic system are important to enhance conversion and yield rates. In this regard, the monolith photoreactors are considered more efficient as the reactors have higher surface area, more catalyst loading and good distribution of light over the catalyst surface due to their microchannels.

In addition, it is important to consider all operating parameters such as initial CO_2 concentration, reaction time, temperature, light intensity, system pressure, pH and activity decay over time during photocatalytic CO_2 reduction. These factors would be helpful to evaluate the average productivity that are missing in majority of the reported studies and are important for complete analysis of CO_2 photoreduction process. Therefore, in future, more research should focus on CO_2 photoreduction scale-up technology for commercial applications.

6. Conclusions

Photocatalysis is a potentially economical and environment friendly technology for sustainable development. In photocatalytic CO_2 reduction, four key factors are essential to be considered for achieving higher conversion and for improving the efficiency of photocatalytic process. The first key factor is the selection of semiconductor catalyst having appropriate band-gap energies. The proper structure of catalyst participates significantly for improving the conversion, yield and selectivity as well as for increasing the rate of reaction. The metal doped catalysts could help to improve recombination times of charges particles. On the other hand, sensitizers and novel catalysts could contribute significantly to improve yield and selectivity. Co-metals and metal-sensitizers are eminent to maximize yield rates. The next factor is the choice of reductant for CO_2 photoreduction. The effectiveness and product selectivity of photocatalytic reactions is achieved by selecting appropriate reductant. Water is most commonly used as reductant in liquid and gas phase, although solubility of CO_2 in water is very low, and water splitting reaction is more favorable than CO_2 reduction. However, during CO_2 reduction with water, three main products including CH_4, CH_3OH and CO could be found if water does not compete with H_2O. On the other hand, CH_4 is a very attractive reductant and supports the production of hydrocarbons, H_2 and CO. Appropriate design of a photocatalytic reactor is the third important factor. The design of photoreactor is different from the conventional chemical reactors and in photocatalysis technology; there is a gap in this research area. Photoreactors are mostly practiced for water and air treatment and each research group has their individual design without any discipline and set criteria. In case of photoreduction of CO_2 to renewable fuels, the conventional available reactors are utilized. The reactor design for increasing the efficiency of CO_2 reduction is lacking as the reactor is incapable of harnessing solar radiations efficiently. However, optical fiber and monolith photoreactor are more suitable for CO_2 reduction applications due to their higher illuminated surface area. Finally, optimizations of the operating conditions are important for engineering and commercialization purposes. Therefore, it is important to consider all operating parameters such as CO_2 concentration, reaction time, temperature, light intensity, system pressure, pH and activity decay for higher conversion and yield rates. The present available phototechnologies are still operating under lower conversion, yield and selectivity. Thus, further research efforts are needed to deliberate all the above four factors for maximum efficiency.

Acknowledgment

The authors would like to extend their deepest appreciation to the Ministry of Higher Education (MOHE) and Universiti Teknologi Malaysia for partial financial support of this research under LRGS (Long-term Research Grant Scheme) and RUG (Research University Grant) research grants, respectively.

References

[1] Ghoniem AF. Needs, resources and climate change: clean and efficient conversion technologies. Progress in Energy and Combustion Science 2011;37:15–51.
[2] Gill SS, Tsolakis A, Dearn KD, Rodríguez-Fernández J. Combustion characteristics and emissions of Fischer–Tropsch diesel fuels in IC engines. Progress in Energy and Combustion Science 2010;37:503–23.
[3] Balat H, Elif K. Hydrogen from biomass—present scenario and future prospects. International Journal of Hydrogen Energy 2010;35:7416–26.
[4] Roy SC, Varghese OK, Paulose M, Grimes CA. Toward solar fuels: photocatalytic conversion of carbon dioxide to hydrocarbons. ACS Nano 2010;4: 1259–78.
[5] Le THN, Tran QV, Nguyen TTL, Van DST, Yang XY, Su BL. Preparation of biofuels by catalytic cracking reaction of vegetable oil sludge. Fuel 2011;90:1069–75.
[6] Yan XY, Crookes RJ. Energy demand and emissions from road transportation vehicles in China. Progress in Energy and Combustion Science 2010;36: 651–76.
[7] Nigam PS, Singh A. Production of liquid biofuels from renewable resources. Progress in Energy and Combustion Science 2011;37:52–68.
[8] Peng J, Lu L, Yang H. Review on life cycle assessment of energy payback and greenhouse gas emission of solar photovoltaic systems. Renewable and Sustainable Energy Reviews 2013;19:255–74.
[9] Chew T, Bhatia S. Catalytic processes towards the production of biofuels in a palm oil and oil palm biomass-based biorefinery. Bioresource Technology 2008;99:7911–22.
[10] Centi G, Lanzafame P, Perathoner S. Analysis of the alternative routes in the catalytic transformation of lignocellulosic materials. Catalysis Today 2011;167:14–30.
[11] Varun Prakash R, Bhat IK. Energy, economics and environmental impacts of renewable energy systems. Renewable and Sustainable Energy Reviews 2009;13:2716–21.
[12] George AO, Alain G, Prakash GKS. Beyond oil and gas: the methanol economy. Los Angeles: Wiley-VCH; 2009.
[13] Panwar NL, Kaushik SC, Kothari S. Role of renewable energy sources in environmental protection: a review. Renewable & Sustainable Energy Reviews 2011;15:1513–24.
[14] Mekhilef S, Siga S, Saidur R. A review on palm oil biodiesel as a source of renewable fuel. Renewable and Sustainable Energy Reviews 2011;15: 1937–49.
[15] Centi G, Santen RAV. Catalysis for renewables. Weimheim: Wiley-VCH; 2007.
[16] Xiaoding X, Moulijn JA. Mitigation of CO_2 by chemical conversion: plausible chemical reactions and promising products. Energy & Fuels 1996;10:305–25.

[17] VijayaVenkataRaman S, Iniyan S, Goic R. A review of climate change, mitigation and adaptation. Renewable and Sustainable Energy Reviews 2012;16:878–97.
[18] Whipple DT, Kenis PJA. Prospects of CO_2 utilization via direct heterogeneous electrochemical reduction. Journal of Physical Chemistry Letters 2010;1:3451–8.
[19] Indrakanti VP, Schobert HH, Kubicki JD. Quantum mechanical modeling of CO_2 interactions with irradiated stoichiometric and oxygen-deficient anatase TiO_2 surfaces: implications for the photocatalytic reduction of CO_2. Energy & Fuels 2009;23:5247–56.
[20] Meshkini F, Taghizadeh M, Bahmani M. Investigating the effect of metal oxide additives on the properties of $Cu/ZnO/Al_2O_3$ catalysts in methanol synthesis from syngas using factorial experimental design. Fuel 2010;89:170–5.
[21] Olah GA, Goepper A, Prakash Surya GK. Beyond oil and gas, the methanol economy. 2nd ed. Los Angeles: Wiley-VCH; 2009.
[22] Zhao T-S, Zhang K, Chen X, Ma Q, Tsubaki N. A novel low-temperature methanol synthesis method from $CO/H_2/CO_2$ based on the synergistic effect between solid catalyst and homogeneous catalyst. Catalysis Today 2010;149:98–104.
[23] Manenti F, Cieri S, Restelli M. Considerations on the steady-state modeling of methanol synthesis fixed-bed reactor. Chemical Engineering Science 2011;66:152–62.
[24] Tao X, Bai M, Wu Q, Huang Z, Yin Y, Dai X. CO_2 reforming of CH_4 by binode thermal plasma. International Journal of Hydrogen Energy 2009;34:9373–8.
[25] Ramaswamy RC, Ramachandran PA, Dudukovic MP. Modeling catalytic partial oxidation of methane to syngas in short-contact-time packed-bed reactors. Industrial Engineering and Chemistry Research 2007;46:8638–51.
[26] Mei H, Li C, Ji S, Liu H. Modeling of a metal monolith catalytic reactor for methane steam reforming-combustion coupling. Chemical Engineering Science 2007;62:4294–303.
[27] Tao X, Bai M, Li X, Long H, Shang S, Yin Y, et al. CH_4–CO_2 reforming by plasma—challenges and opportunities. Progress in Energy and Combustion Science 2011;37:113–24.
[28] Nozaki T, Ağıral A, Yuzawa S, Han Gardeniers JGE, Okazaki K. A single step methane conversion into synthetic fuels using microplasma reactor. Chemical Engineering Journal 2011;166:288–93.
[29] Long H, Shang S, Tao X, Yin Y, Dai X. CO_2 reforming of CH_4 by combination of cold plasma jet and Ni/[gamma]–Al_2O_3 catalyst. International Journal of Hydrogen Energy 2008;33:5510–5.
[30] Li D, Li X, Bai M, Tao X, Shang S, Dai X, et al. CO_2 reforming of CH_4 by atmospheric pressure glow discharge plasma: a high conversion ability. International Journal of Hydrogen Energy 2009;34:308–13.
[31] Carneiro JT, Yang C-C, Moulijn JA, Mul G. The effect of water on the performance of TiO_2 in photocatalytic selective alkane oxidation. Journal of Catalysis 2011;277:129–33.
[32] Wang Z-Y, Chou H-C, Wu JCS, Tsai DP, Mul G. CO_2 photoreduction using NiO/$InTaO_4$ in optical-fiber reactor for renewable energy. Applied Catalysis A: General 2010;380:172–7.
[33] Naik B, Martha S, Parida KM. Facile fabrication of Bi_2O_3/TiO_2-xNx nanocomposites for excellent visible light driven photocatalytic hydrogen evolution. International Journal of Hydrogen Energy 2011;36:2794–802.
[34] Wang C, Thompson RL, Baltrus J, Matranga C. Visible light photoreduction of CO_2 using $CdSe/Pt/TiO_2$ heterostructured catalysts. Journal of Physical Chemistry Letters 2010;1:48–53.
[35] Indrakanti VP, Schobert HH, Kubicki JD. Quantum mechanical modeling of CO_2 interactions with irradiated stoichiometric and oxygen-deficient anatase TiO_2 surfaces: implications for the photocatalytic reduction of CO_2. Energy Fuels 2009;23:5247–56.
[36] Zhao Z, Fan J, Liu S, Wang Z. Optimal design and preparation of titania-supported CoPc using sol–gel for the photo-reduction of CO_2. Chemical Engineering Journal 2009;151:134–40.
[37] Kuramochi T, Ramírez A, Turkenburg W, Faaij A. Techno-economic prospects for CO_2 capture from distributed energy systems. Renewable and Sustainable Energy Reviews 2013;19:328–47.
[38] Mani F, Peruzzini M, Stoppioni P. CO_2 absorption by aqueous NH_3 solutions: speciation of ammonium carbamate, bicarbonate and carbonate by a 13C NMR study. Green Chemistry 2006;8:995.
[39] Graves C, Ebbesen SD, Mogensen M, Lackner KS. Sustainable hydrocarbon fuels by recycling CO_2 and H_2O with renewable or nuclear energy. Renewable and Sustainable Energy Reviews 2011;15:1–23.
[40] Kabra Kavita, Chaudhary Rubina, Sawhney RL. Treatment of hazardous organic and inorganic compounds through aqueous-phase photocatalysis: a review. Industrial Enginnering and Chemistry Research 2004;43:7683–96.
[41] Hd Lasa, Serrano B, Salaices M. Photocatalytic reaction engineering. New York: Springer; 2005.
[42] Arakawa H, Aresta M, Armor JN, Barteau MA, Beckman EJ, Bell AT, et al. Catalysis research of relevance to carbon management: progress, challenges, and opportunities. Chemical Review 2001;101:953–96.
[43] Rayner CM. The potential of carbon dioxide in synthetic organic chemistry. Organic Process Research & Development 2007;11:121–32.
[44] Sakakura Toshiyasu, Choi Jun-Chul, Hiroyuki Yasuda. Transformation of carbon dioxide. Chemical Reviews 2007;107:2365–87.
[45] Clark JH, Tavener SJ. Alternative solvents: shades of green. Organic Process Research & Development 2007;11:149–55.
[46] Halmann M. Photoelectrochemical reduction of aqueous carbon dioxide on p-type gallium phosphide in liquid junction solar cells. Nature 1978;275: 115–6.
[47] Inoue T, Akira F, Satoshi K, Kenichi H. Photoelectrocatalytic reduction of carbon dioxide in aqueous suspensions of semiconductor powders. Nature 1979;277:637–8.
[48] Halmann M, Ulman M, Blajeni BA. Photochemical solar collector for the photoassisted reduction of aqueous carbon dioxide. Solar Energy 1983;31: 429–31.
[49] Anpo M, Chiba K. Photocatalytic reduction of CO_2 on anchored titanium-oxide catalysts. Journal of Molecular Catalysis 1992;74:207–12.
[50] Adachi K, Ohta K, Mizuno T. Photocatalytic reduction of carbon dioxide to hydrocarbons using copper loaded titanium dioxide. Solar Energy Materials and Solar Cells 1994;53:187–90.
[51] Anpo M, Yamashita H, Ichihashi Y, Fujii Y, Honda M. Photocatalytic reduction of CO_2 with H_2O on titanium oxides anchored within micropores of zeolites: effects of the structure of the active sites and the addition of Pt. Journal of Physical Chemistry B 1997;101:2632–6.
[52] Ikeue K, Nozaki S, Ogawa M, Anpo M. Photocatalytic reduction of CO_2 with H_2O on Ti containing porous silicathin film photocatalys. Catalysis Letters 2002;80:111–4.
[53] Sasirekha N, Basha SJS, Shanthi K. Photocatalytic performance of Ru doped anatase mounted on silica for reduction of carbon dioxide. Applied Catalysis B: Environmental 2006;62:169–80.
[54] Liou PY, Chen SC, Wu JCS, Liu D, Mackintosh S, Maroto-Valer M, et al. Photocatalytic CO_2 reduction using an internally illuminated monolith photoreactor. Energy & Environmental Science 2011;4:1487–94.
[55] Sato S, Arai T, Morikawa T, Uemura K, Suzuki TM, Tanaka H, et al. Selective CO_2 conversion to formate conjugated with H_2O oxidation utilizing semi-conductor/complex hybrid photocatalysts. Journal of the American Chemical Society 2011;133:15240–3.
[56] Zhou Y, Tian Z, Zhao Z, Liu Q, Kou J, Chen X, et al. High-yield synthesis of ultrathin and uniform Bi_2WO_6 square nanoplates benefitting from photocatalytic reduction of CO_2 into renewable hydrocarbon fuel under visible light. ACS Applied Matererials and Interfaces 2011;3:3594–601.
[57] Tsai CW, Chen HM, Liu RS, Asakura K, Chan TS. Ni@NiO core–shell structure-modified nitrogen-doped $InTaO_4$ for solar-driven highly efficient CO_2 reduction to methanol. Journal of Physical Chemistry C 2011;115: 10180–6.
[58] Li X, Li W, Zhuang Z, Zhong Y, Li Q, Wang L. Photocatalytic reduction of carbon dioxide to methane over SiO_2-pillared HNb_3O_8. The Journal of Physical Chemistry C 2012;116:16047–53.
[59] Yadav RK, Baeg JO, Oh GH, Park NJ, Kong KJ, Kim J, et al. A photocatalyst-enzyme coupled artificial photosynthesis system for solar energy in production of formic acid from CO_2. Journal of the American Chemical Society 2012;134:11455–61.
[60] An C, Wang J, Jiang W, Zhang M, Ming X, Wang S, et al. Strongly visible-light responsive plasmonic shaped AgX: Ag (X=Cl, Br) nanoparticles for reduction of CO_2 to methanol. Nanoscale 2012;4:5646–50.
[61] Tseng I-Hsiang, Chang Wan-Chen, WJ CS. Photoreduction of CO_2 using sol–gel derived titania and titania-supported copper catalysts. Applied Catalysis B: Environmental 2002;37:37–48.
[62] Slamet Nasution HW, Purnama E, Kosela S, Gunlazuardi J. Photocatalytic reduction of CO_2 on copper-doped titania catalysts prepared by improved-impregnation method. Catalysis Communications 2005;6:313–9.
[63] Wu JCS. Photocatalytic reduction of greenhouse gas CO_2 to fuel. Catalysis Syrveys from Asia 2009;13:30–40.
[64] Hou W, Hung WH, Pavaskar P, Goeppert A, Aykol M, Cronin SB. Photocatalytic conversion of CO_2 to hydrocarbon fuels via plasmon-enhanced absorption and metallic interband transitions. ACS Catalysis 2011;1: 929–36.
[65] Zhang QY, Li Y, Ackerman EA, Gajdardziska-Josifovska M, Li HL. Visible light responsive iodine-doped TiO_2 for photocatalytic reduction of CO_2 to fuels. Applied Catalysis A: General 2011;400:195–202.
[66] Tatsuto Yui, Akira Kan, Chieko Saitoh, Azuhide K, Takashi Ibusuki, Osamu I. Photochemical reduction of CO_2 using TiO_2: effects of organic adsorbates on TiO_2 and deposition of Pd onto TiO_2. ACS Applied Materials & Interfaces 2011;3:2594–600.
[67] Ozcan O, Yukruk F, Akkaya EU, Uner D. Dye sensitized CO_2 reduction over pure and platinized TiO_2. Topics in Catalysis 2007;44:523–8.
[68] Wang Q, Wu W, Chen J, Chu G, Ma K, Zou H. Novel synthesis of $ZnPc/TiO_2$ composite particles and carbon dioxide photo-catalytic reduction efficiency study under simulated solar radiation conditions. Colloids and Surfaces A: Physicochemical and Engineering Aspects 2012;409:118–25.
[69] Maomingren Ravikrishna, Valsaraj K. Photocatalytic degradation of gaseous organic species on photonic band-gap titania. Environmental Science and Technology 2006;40:7029–33.
[70] Zhang Y-Q, Zhou W, Liu S, Navrotsky A. Controllable morphology of engelhard titanium silicates ETS-4: synthetic, photocatalytic, and calorimetric studies. Chemistry of Materials 2011;23:1166–73.
[71] Guan GQ, Kida T, Yoshida A. Reduction of carbon dioxide with water under concentrated sunlight using photocatalyst combined with Fe-based catalyst. Applied Catalysis B: Environmental 2003;41:387–96.
[72] Liu S, Guo E, Yin L. Tailored visible-light driven anatase TiO_2 photoctalysts based on controlable metal ion doping and ordered mesoporous structure. Journal of Materials Chemistry 2012;22:5031–41.
[73] Xia XH, Jia ZH, Yu Y, Liang Y, Wang Z, Ma LL. Preparation of multi-walled carbon nanotube supported TiO_2 and its photocatalytic activity in the reduction of CO_2 with H_2O. Carbon 2007;45:717–21.

[74] Ai ZH, Ho WK, Lee S. Efficient visible light photocatalytic removal of NO with BiOBr-graphene nanocomposites. Journal of Physical Chemistry C 2011;115: 25330–7.
[75] Woolerton TW, Sheard S, Pierce E, Ragsdale SW, Armstrong FA. CO_2 photoreduction at enzyme-modified metal oxide nanoparticles. Energy & Environmental Science 2011;4:2393–9.
[76] Ettedgui J, Diskin-Posner Y, Weiner L, Neumann R. Photoreduction of carbon dioxide to carbon monoxide with hydrogen catalyzed by a rhenium (I) phenanthroline–polyoxometalate hybrid complex. Journal of the American Chemical Society 2010;133:188–90.
[77] Anpo M, Yamashita H, Ichihashi Y, Ehara S. Photocatalytic reduction of CO_2 with H_2O on various titanium-oxide catalysts. Journal of Electroanalytical Chemistry 1995;396:21–6.
[78] Kaneco Satoshi, Kurimoto Hidekazu, Ohta Kiyohisa, Mizuno Takayuki, Saji A. Photocatalytic reduction of CO_2 using TiO_2, powders in liquid CO_2 medium. Journal of Photochemistry and Photobiology A: Chemistry 1997;109:59–63.
[79] Hinogami R, Nakamura Y, Yae S, Nakato Y. An approach to ideal semiconductor electrodes for efficient photoelectrochemical reduction of carbon dioxide by modification with small metal particles. Journal of Physical Chemistry B 1998;102:974–80.
[80] Anpo M, Yamashita H, Ikeue K, Fujii Y, Zhang SG, Ichihashi Y, et al. Photocatalytic reduction of CO_2 with H_2O on Ti-MCM-41 and Ti-MCM-48 mesoporous zeolite catalysts. Catalysis Today 1998;44:327–32.
[81] Kohno Y, Hayashi H, Takenaka S, Tanaka T, Funabiki T, Yoshida S. Photo-enhanced reduction of carbon dioxide with hydrogen over Rh/TiO_2. Journal of Photochemistry and Photobiology A: Chemistry 1999;126:117–23.
[82] Ikeue K, Nozaki S, Ogawa M, Anpo M. Characterization of self-standing Ti-containing porous silica thin films and their reactivity for the photocatalytic reduction of CO_2 with H_2O. Catalysis Today 2002;74:241–8.
[83] Shioya Y, Ikeue K, Ogawa M, Anpo M. Synthesis of transparent Ti-containing mesoporous silica thin film materials and their unique photocatalytic activity for the reduction of CO_2 with H_2O. Applied Catalysis A: General 2003;254:251–9.
[84] Hwang J-S, Chang J-S, Park S-E, Ikeue K, Anpo M. High performance photocatalytic reduction of CO_2 with H_2O by TiSBA-15 mesoporous material. Studies in Surface Science and Catalysis 2004;153:299–302.
[85] Shi D, Feng Y, Zhong S. Photocatalytic conversion of CH_4 and CO_2 to oxygenated compounds over $Cu/CdS–TiO_2/SiO_2$ catalyst. Catalysis Today 2004;98:505–9.
[86] Dey GR, Belapurkar AD, Kishore K. Photo-catalytic reduction of carbon dioxide to methane using TiO_2 as suspension in water. Journal of Photochemistry and Photobiology A: Chemistry 2004;163:503–8.
[87] Kentaro T, Tsunehiro T, Haruka I, Yoshiumi K, Takuzo F. Photocatalytic reduction of CO_2 to CO in the presence of H_2 or CH_4 as a reductant over MgO. Journal of Physical Chemistry B 2004;108:346–54.
[88] Wu JCS, Lin HM, Lai CL. Photoreduction of CO_2 to methanol using optical-fiber photoreactor. Applied Catalysis A: General 2005;296:194–200.
[89] Hiromi Yamashita, Miho Okazaki, Ikeue K, Anpo M. Photocatalytic reduction of CO_2 with H_2O on Ti containing mesoporous silica hydrophobically modified using fluoride ions. Studies in Surface Science and Catalysis 2004;153:289–94.
[90] Tan SS, Zou L, Hu E. Photocatalytic reduction of carbon dioxide into gaseous hydrocarbon using TiO_2 pellets. Catalysis Today 2006;115:269–73.
[91] Usubharatana P, McMartin D, Veawab A, Tontiwachwuthikul P. Photocatalytic process for CO_2 emission reduction from industrial flue gas streams. Industrial & Engineering Chemistry Research 2006;45:2558–68.
[92] Lo C-C, Hung C-H, Yuan C-S, Wu J-F. Photoreduction of carbon dioxide with H_2 and H_2O over TiO_2 and ZrO_2 in a circulated photocatalytic reactor. Solar Energy Materials and Solar Cells 2007;91:1765–74.
[93] Pan PW, Chen YW. Photocatalytic reduction of carbon dioxide on $NiO/InTaO_4$ under visible light irradiation. Catalysis Communications 2007;8:1546–9.
[94] Yuliati L, Itoh H, Yoshida H. Photocatalytic conversion of methane and carbon dioxide over gallium oxide. Chemical Physics Letters 2008;452:178–82.
[95] Nguyen TV, Wu JCS. Photoreduction of CO_2 in an optical-fiber photoreactor: effects of metals addition and catalyst carrier. Applied Catalysis A: General 2008;335:112–20.
[96] Tan SS, Zou L, Hu E. Kinetic modelling for photosynthesis of hydrogen and methane through catalytic reduction of carbon dioxide with water vapour. Catalysis Today 2008;131:125–9.
[97] Mishra UK. Semiconductor device physics and design. Netherlands: Springer; 2008.
[98] Kuwahara Y, Kamegawa T, Mori K, Matsumura Y, Yamashita H. Fabrication of hydrophobic zeolites using triethoxyfluorosilane and their application for photocatalytic degradation of acetaldehyde. Topics in Catalysis 2009;52:643–8.
[99] Kocı K, Obalova L, Matejova L, Placha D, Lacny Z, Jirkovsky J, et al. Effect of TiO_2 particle size on the photocatalytic reduction of CO_2. Applied Catalysis B: Environmental 2009;89:494–502.
[100] Wang ZY, Chou HC, Wu JCS, Tsai DP, Mul G. CO_2 photoreduction using $NiO/InTaO_4$ in optical-fiber reactor for renewable energy. Applied Catalysis A: General 2010;380:172–7.
[101] Li Y, Wang WN, Zhan ZL, Woo MH, Wu CY, Biswas P. Photocatalytic reduction of CO_2 with H_2O on mesoporous silica supported Cu/TiO_2 catalysts. Applied Catalysis B: Environmental 2010;100:386–92.
[102] Kočí K, Matějů K, Obalová L, Krejčíková S, Lacný Z, Plachá D, et al. Effect of silver doping on the TiO_2 for photocatalytic reduction of CO_2. Applied Catalysis B: Environmental 2010;96:239–44.
[103] Kočí K, Reli M, Kozák O, Lacný Z, Plachá D, Praus P, et al. Influence of reactor geometry on the yield of CO_2 photocatalytic reduction. Catalysis Today 2011;176:212–4.
[104] Asi AM, Chun H, Minhua S, Dehua X, Long L, Huiqi D, et al. Photocatalytic reduction of CO_2 to hydrocarbons using $AgBr/TiO_2$ nanocomposites under visible light. Catalysis Today 2011;175:256–63.
[105] Indrakanti VP, Kubickib JD, Schobert HH. Photoinduced activation of CO_2 on Ti-based heterogeneous catalysts: current state, chemical physics-based insights and outlook. Energy & Environmental Science 2009;2:745–58.
[106] Yahaya AH, Gondal MA, Hameed A. Selective laser enhanced photocatalytic conversion of CO_2 into methanol. Chemical Physics Letters 2004;400:206–12.
[107] Lehn JM, Ziessel R. Photochemical generation of carbon monoxide and hydrogen by reduction of carbon dioxide and water under visible light irradiation. Proceedings of the National Academy of Sciences of the United States of America 1982;79:701–4.
[108] Zhao C, Krall A, Zhao H, Zhang Q, Li Y. Ultrasonic spray pyrolysis synthesis of Ag/TiO_2 nanocomposite photocatalysts for simultaneous H_2 production and CO_2 reduction. International Journal of Hydrogen Energy 2012;37:9967–76.
[109] Yang XY, Xiao TC, Edwards PP. The use of products from CO_2 photoreduction for improvement of hydrogen evolution in water splitting. International Journal of Hydrogen Energy 2011;36:6546–52.
[110] Linsebigler AL, Lu G, Yates Jr. JT. Photocatalysis on TiO_2 surfaces: principles, mechanisms, and selected results. Chemical Reviews 1995;95:735–58.
[111] Aliwi SM, Al-Jubori KF. Photoreduction of CO_2 by metal sulphide semiconductors in presenceof H_2S. Solar Energy Materials 1989;18:223–9.
[112] Inoue H, Moriwaki H, Maeda K, Yoneyama H. Photoreduction of carbon-dioxide using chalcogenide semiconductor microcrystals. Journal of Photochemistry and Photobiology A: Chemistry 1995;86:191–6.
[113] Anpo M, Yamashita H, Yi Ichihash, Ehara S. Photocatalytic reduction of CO_2 with H_2O on various titanium oxide catalysts. Journal of Electroanalytical Chemistry 1995;396:21–6.
[114] la CDd, Arévalo JC, Torres G, Margulis RGB, Ornelas C, Aguilar-Elguézabal A. TiO_2 doped with Sm^{3+} by sol–gel: synthesis, characterization and photocatalytic activity of diuron under solar light. Catalysis Today 2011;166:152–8.
[115] Guaraldo TT, Pulcinelli SH, Zanoni MVB. Influence of particle size on the photoactivity of Ti/TiO_2 thin film electrodes, and enhanced photoelectrocatalytic degradation of indigo carmine dye. Journal of Photochemistry and Photobiology A: Chemistry 2011;217:259–66.
[116] Srinivasan SS, Wade J, Stefanakos EK, Goswami Y. Journal of Alloys and Compounds 2006;424:322–6.
[117] Cong Y, Zhang JL, Chen F, Anpo M, He DN. Preparation, photocatalytic activity, and mechanism of nano-TiO_2 Co-doped with nitrogen and iron (III). Journal of Physical Chemistry C 2007;111:10618–23.
[118] Mori K, Yamashita H, Anpo M. Photocatalytic reduction of CO_2 with H_2O on various titanium oxide photocatalysts. RSC Advances 2012;2:3165.
[119] Anpo M. Approach to photocatalysis at the molecular level design of photocatalysts, detection of intermediate species, and reaction mechanisms. Solar Energy Materials and Solar Cells 1995;38:221–38.
[120] Keita Ikeue, Hiromi Yamashita, Masakazu Anpo. Photocatalytic reduction of CO_2 with H_2O on Ti-zeolite photocatalysts: effect of the hydrophobic and hydrophilic properties. Journal of Physical Chemistry B 2001;105:8350–5.
[121] Ikeue K, Nozaki S, Ogawa M, Anpo M. Characterization of self-standing Ti-containing porous silica thin films and their reactivity for the photocatalytic reduction of CO_2 with H_2O. Catalysis Today 2002;74:241–8.
[122] Hiromi Y, Akira S, Kawasaki S-i, Yuichi I, Shaw E, Masakazu A. Photocatalytic synthesis of CH_4 and CH_3OH from CO_2 and H_2O on highly dispersed active titanium oxide catalysts. Energy Conversion and Management 1995;36: 617–20.
[123] Le TT, Akhtar MS, Park DM, Lee JC, Yang OB. Water splitting on Rhodamine-B dye sensitized Co-doped TiO_2 catalyst under visible light. Applied Catalysis B: Environmental 2012;111:397–401.
[124] Li X, Liu HL, Luo DL, Li JT, Huang Y, Li HL, et al. Adsorption of CO_2 on heterostructure $CdS(Bi_2S_3)/TiO_2$ nanotube photocatalysts and their photocatalytic activities in the reduction of CO_2 to methanol under visible light irradiation. Chemical Engineering Journal 2012;180:151–8.
[125] Braham RJ, Harris AT. Review of major design and scale-up considerations for solar photocatalytic reactors. Industrial & Engineering Chemistry Research 2009;48:8890–905.
[126] Halmann M, Katzir V. Photoassisted carbon dioxide reduction on aqueous suspensions of titanium dioxide. Solar Energy Materials 1984;10:85–91.
[127] Yamashita H, Kawasaki S, Takeuchi M, Fujii Y, Ichihashi Y, Suzuki Y, et al. Photocatalytic reduction of CO_2 with H_2O on Ti/Si binary oxide catalysts prepared by the sol–gel method. Advances in Chemical Conversions for Mitigating Carbon Dioxide 1998;114:561–4.
[128] Imoberdorf GE, Cassano AE, Irazoqui HA, Alfano OM. Optimal design and modeling of annular photocatalytic wall reactors. Catalysis Today 2007;129: 118–26.
[129] Ling CM, Mohamed AR, Bhatia S. Performance of photocatalytic reactors using immobilized TiO_2 film for the degradation of phenol and methylene blue dye present in water stream. Chemosphere 2004;57:547–54.
[130] Tomašić V, Jović F, Gomzi Z. Photocatalytic oxidation of toluene in the gas phase: modelling an annular photocatalytic reactor. Catalysis Today 2008;137: 350–6.
[131] Vincent G, Marquaire PM, Zahraa O. Abatement of volatile organic compounds using an annular photocatalytic reactor: study of gaseous acetone. Journal of Photochemistry and Photobiology A: Chemistry 2008;197:177–89.

[132] Du P, Cameiro JT, Moulijn JA, Mul G. A novel photocatalytic monolith reactor for multiphase heterogeneous photocatalysis. Applied Catalysis A: General 2008;334:119–28.
[133] Puma GL, Yue PL. A novel fountain photocatalytic reactor: model development and experimental validation. Chemical Engineering Science 2001;56: 2733–44.
[134] Cassano AE, Alfano OM. Reaction engineering of suspended solid heterogeneous photocatalytic reactor. Catalysis Today 2000;58:167–97.
[135] Zhang Z, Anderson W, Mooyoung M. Experimental analysis of a corrugated plate photocatalytic reactor. Chemical Engineering Journal 2004;99:145–52.